UPPSALA
UNIVERSITET

UPTEC E 25010
Examensarbete 30 hp
Juni 2025

Harmonics' effect on electrical equipment at hydropower plants

A study on the current situation regarding harmonics at hydropower plants and the challenges with measuring voltage harmonics

Axel Eriksson

Civilingenjörsprogrammet i elektroteknik

UPPSALA UNIVERSITET

Harmonics' effects on electrical equipment in hydro power plants

Axel Eriksson

Abstract

This thesis investigates how voltage and current harmonics can affect electrical equipment at hydropower plants. A review was conducted to examine both the impact of voltage and current harmonics on electrical equipment and the challenges with measuring voltage harmonics at higher voltage levels. To further support this investigation, harmonic measurements have been carried out at four hydropower plants.

The findings from the analyzed data show that harmonic levels in the grids connecting hydropower plants are generally low. However, harmonic distortions generated by sources several kilometers away, such as wind farms, were detectable. The study also highlights the limitations of using conventional measurement transformers for measuring voltage harmonics. While inductive voltage transformers may provide acceptable accuracy up to a few kilohertz at lower voltage levels, significant errors can occur at higher voltages and frequencies due to resonance. Capacitive voltage transformers cannot be used for harmonic measurements due to their precise tuning around a specific frequency. Three alternative methods for measuring voltage harmonics are presented in this thesis.

A fairly new concern in the electrical grid is the presence of supraharmonics, harmonic components with frequencies between 2 kHz and 150 kHz. These can, for example, be created by frequency converters connected to the grid. To be able to measure these high frequency voltages, special methods with a large frequency range are required. This thesis also investigates potential issues with supraharmonics in hydropower plants. Identified issues include increased losses and failures in cable terminations. However, the risk due to supraharmonics might be small today but may increase if more frequency converters are connected in the proximity of hydropower plants.

Teknisk-naturvetenskapliga fakulteten

Uppsala universitet, Utgivningsort Uppsala

Handledare: Robert Bronegård, Fortum Sverige AB Ämnesgranskare: Urban Lundin

Examinator: Saman Majdi

POPULÄRVETENSKAPLIG SAMMANFATTNING

Sveriges elsystem har under de senaste årtiondena genomgått stora förändringar med en ökad andel av förnybar elproduktion i form av framför allt vind- och solkraft. Dessa energislag ansluts idag till elnäten med omriktare på ett eller annat sätt, vilket kan skapa nya utmaningar i elsystemet. Omriktare är olinjära komponenter vars ström inte är proportionell mot spänningen, något som skapar övertoner. En modern omriktare kan ha en switchfrekvens på flera kilohertz vilket kan skapa övertoner vid denna frekvens samt vid multiplar av denna.

Övertoner har alltid förekommit i elnätet, roterande maskiner och transformatorer är två typer av elektrisk utrustning på mellan- och högspänningsnivån som kan orsaka dessa. Dessa övertoner innehåller främst frekvenser upp till ett fåtal kilohertz. För höga nivåer av övertoner kan orsaka problem i elsystemet såsom ökade förluster, ökat slitage, problem med reläskydd och i värsta fall haverier. Supratoner är övertoner med en frekvens mellan 2 kHz och 150 kHz och orsakas främst av switchfrekvensen från omriktare. Den här typen av övertoner orsakar främst problem på lågspänningsnivån men kan även orsaka problem på högre spänningsnivåer.

För att kunna upptäcka dessa högfrekventa övertoner krävs speciell mätutrustning. Att mäta på traditionella mättransformatorer ger ofta en dålig noggrannhet då utrustningen inte är konstruerade för att mäta frekvenser över den fundamentala. I induktiva mättransformatorer skapas resonans mellan lindningar vilket både kan förstärka och försvaga den uppmätta högfrekventa signalen. Oftast ger den här typen av mättransformator en acceptabel noggrannhet upp till ett fåtal kilohertz, det kan däremot variera mycket beroende på typ och spänningsnivå. Kapacitiva mättransformatorer kan inte användas för övertonsmätningar då dessa redan vid ett par hundra Hertz kan ge stora mätfel. För att kunna mäta övertoner på högre spänningsnivåer krävs därför andra metoder. Tre förslag på metoder presenteras i det här arbetet.

Övertoner kan som tidigare nämnt kan orsaka problem i elektrisk utrustning där ett av de största problemen är ökade värmeförluster. Många av dessa värmeförluster är också frekvensberoende vilket gör att även en överton med låg amplitud fast med hög frekvens kan skapa betydande förluster. Dessa värmeförluster kan orsakas av både ström och spänningsövertoner. Kabelavslut för mellanspänningsapplikationer har visat sig vara känsliga för spänningssupratoner. Även transformatorer anslutna till stora olinjära laster kan drabbas negativt med en förkortad livslängd som ett resultat.

I detta arbete har mätningar av spänningsövertoner upp till den 49:e övertonen gjorts vid tre vattenkraftverk och det visar att nivåerna av övertoner är låga. Däremot gjordes dessa mätningar på befintliga mättransformatorer vilket har begränsat noggrannheten, framför allt vid högre frekvenser. Det var däremot möjligt att se vissa mönster av hur övertonshalten förändras över tid. Under vardagar kunde en tydlig ökning observeras vid två av kraftverken och vid ett av dessa kraftverk kunde även övertoner kopplade till en vindkraftpark observeras.

ACKNOWLEDGEMENTS

This master’s thesis is the final chapter of my studies in the master's program in Electrical Engineering at Uppsala University. I am grateful for the opportunity to conduct my thesis in collaboration with Fortum since it gave me the chance to meet knowledgeable people who gave me unique experiences of learning about hydropower from the inside. Thank you to everyone at Fortum for the experience!

There are a few people I would like to give special thanks to. Firstly, a special thanks to my industrial supervisor, Robert Bronegård, and my managers, Hans Bjerhag and Karar Al Obeid. Your support and feedback throughout the project have been truly invaluable, and I have learned a lot from all of you! I am also grateful to John, Conny, Tomas, and Niclas for guiding me around the hydropower plants during my measurements. A big thank you also goes out to all the other master’s thesis students at Fortum, your companionship made this experience not only educational but also a lot more fun!

Finally, I want to thank everyone outside of Fortum who supported me in various ways, from assistance with measurement equipment and data to providing theoretical advice. A special thanks to David Berg at Falu Energi & Vatten for lending me measurement equipment and literature, and for helping me connect with knowledgeable experts.

June 2025, Uppsala

Axel Eriksson

ABBREVIATIONS

CT – Current transformer

CVT – Capacitive voltage transformer

DFIG – Double-fed induction generator

DFT – Discrete Fourier Transform

EHV – Extra high voltage

EMC – Electromagnetic compatibility

EMU – Electromagnetic unit

FFT – Fast Fourier Transform

HPP – Hydropower plant

HV – High voltage

IEC – International Electrotechnical Commission

IEEE – Institute of Electrical and Electronics Engineers

IVT – Inductive voltage transformer

LV – Low voltage

MV – Medium voltage

PMSG – Permanent magnet synchronous generator

PWM – Pulse width modulation

RCVD – Resistive capacitive voltage divider

RMS – Root Mean Square

THD – Total harmonic distortion

TABLE OF CONTENTS

1 INTRODUCTION

The Swedish electrical power system is complex with many different parts. Historically, the majority of the electricity production in Sweden came from hydropower, mainly from the rivers in the north combined with some thermal and nuclear power located further south. These sources relied on synchronous generators that were connected directly to the grid. Over the years, the demand from consumers for more renewable and clean electricity has increased, but hydropower cannot be expanded more for several reasons. More nuclear power has not yet been built; however, this might change in the future. Renewable energy sources such as wind- and solar power have therefore become a more important source of electricity (Energimyndigheten, 2023). These sources are generally not connected directly to the grid, as they often produce either DC voltage or AC voltage with incorrect frequency for the grid. Wind turbines can be connected directly to the grid if they are designed to operate at a constant speed. However, modern wind turbines typically spin at variable speeds depending on wind conditions, resulting in an AC output with varying amplitude and frequency. To integrate such energy sources into the grid, frequency converters are required to produce a stable sinusoidal waveform with the correct grid frequency (Kroposki, 2024). Large loads with frequency converters are also becoming more common in the system. A frequency converter generates a specific waveform by using power electronics to perform precise switching in a specific manner. This controlled switching can introduce distortions in the current, resulting in a waveform that includes not only the fundamental sinusoidal frequency but also harmonics. Traditionally, harmonics up to a few kilohertz have been the predominant type in the power system. However, with the high switching frequency of modern frequency converters, harmonics with frequencies reaching tens of kilohertz can now be observed.

The Electromagnetic Compatibility (EMC) directive exists to ensure that harmonic levels in the grid remain sufficiently low. The directive ensures that electrical equipment does not interfere with other devices. Virtually all electrical equipment must comply with the regulations set by this directive, with a few exceptions (Elsäkerhetsverket, 2025). Many of the relevant standards concerning harmonics in power systems can be found in the IEC 61000 series, and several of these will be referenced in this thesis (Wiid and van der Merwe, 2007).

Harmonics can increase losses in electrical conductors, iron cores, and insulation materials in the power system. These losses are often frequency dependent, meaning that harmonics with a high-frequency can generate more losses, even if the amplitudes are the same. These additional heat losses can lead to overheating, reduced efficiency, and potential equipment failure. Hydroelectric power has been around in Sweden for over a century, and much of the electrical equipment in the hydropower plants (HPPs) has been in operation for many decades. Therefore, it may not have been designed for today's grids with a growing portion of frequency converters and these new types of harmonics. These high-frequency harmonics can even cause failures of vital equipment resulting in expensive outages (Rajkumar, Balasubramanian and Kathirvelu, 2024). It is therefore of interest to Fortum to know if this can be a problem in its HPPs.

Measurements need to be performed to confirm whether any harmonic issues are present. However, due to the high voltage levels, special techniques are required. Conventional measurement transformers are limited to measurements of the fundamental frequency only and

are not suitable to measure the switching frequencies used by modern frequency converters. It may therefore be a risk that harmful high-frequency harmonics are present with no way of detecting them before it is too late, and a failure occurs.

1.1 PURPOSE

The purpose of this thesis is to investigate the current harmonic condition at some of Fortum's HPPs, and how these harmonics can be measured in a practical way with good accuracy. Supraharmonics are a relatively new issue that has not been thoroughly investigated. Supraharmonics are harmonics in a frequency range from 2 kHz to 150 kHz. Thus, there is an interest in investigating how these harmonics could affect electrical equipment at HPPs, as well as how these can be measured. This study will be conducted through a literature review combined with measurements of harmonics at HPPs. All the measurement data will be used to determine whether there are any issues due to harmonics at Fortum's HPPs and at the same time identify if there is any correlation between voltage harmonic levels and other parameters in the grid, such as wind power production.

1.2 PROBLEM FORMULATION

The challenge in this master's thesis is to perform measurements with high enough accuracy to be able to draw conclusions on the levels of voltage harmonics at the HPPs. This thesis will give an answer whether there are any specific or general issues with harmonics at some of Fortum's HPPs. A review on how voltage harmonics could be measured in a practical way on voltage levels above one kilovolt and up into the supraharmonic frequencies will also be given. Finally, the thesis will illuminate the impact of large quantities of harmonics on electrical equipment in the proximity of HPPs.

The research questions guiding this study are:

RQ1. How can harmonics be a problem for electrical equipment at HPPs?

RQ2. How could harmonics and supraharmonics be measured on site in a practical way?

RQ3. How do the voltage harmonic levels at HPPs vary during a week?

1.3 DELIMITATIONS

This report considers only harmonics, excluding other power quality issues. Due to limitations of measurement equipment, only voltage harmonics up to a frequency of maximum 2.5 kHz will be measured. A balanced three-phase system will be assumed with equal amounts of harmonics in each phase. Only voltage harmonics from the weekly measurements will be evaluated; current will, however, be measured if possible. The phase angles of the harmonics will also be disregarded in this thesis, hence only the amplitudes will be regarded.

1.4 REPORT STRUCTURE

Section 2 provides a theoretical background on relevant topics such as equipment in a HPP, what harmonics are, and how they can cause problems. A deeper explanation of how harmonics can be measured will also be given. This includes an explanation of the limitations of using

regular measurement transformers for harmonic measurement as well as a presentation of a few alternatives.

In Section 3, a review of supraharmonics will be provided. This will include their sources, how they propagate in the grid, and how these can be an issue at HPPs. Section 4 outlines the measurement methodology and locations. The results are presented in Section 5 and can be divided into two sections. The first and most comprehensive part is the voltage measurements and their levels against a standard. The second part is less comprehensive and consists of a current measurement from a battery storage system. A presentation of measurement errors will also be presented in this section.

Discussion of the obtained results from the measurements and review is given in Section 6. Additionally, recommendations for future work will be presented. The conclusion from this thesis is then given in Section 7.

2 THEORETICAL BACKGROUND

The theoretical background explains the underlying theory necessary to understand the contents of this thesis. The theoretical background covers the electrical system, including vital electrical equipment. It will explain harmonics, how to measure them, and their potential issues at a HPP.

2.1 ELECTRICITY SYSTEM

This section provides an overview of the Swedish electricity system, with a focus on how grids with different voltage levels are connected within the system.

2.1.1 Electricity grid

Sweden, Norway, Finland and eastern Denmark are synchronously connected in one large grid, meaning that all of these countries have the same system frequency. In this area and in the rest of Europe, the system frequency is 50 Hz. This grid is also connected to other countries via high-voltage direct current (HVDC) connections enabling two different grids to be connected without being synchronously connected. The AC grid in Sweden consists of multiple parts with different voltage levels and purposes. On the highest voltage levels, the transmission grid can be found, which has a nominal voltage from 220 kV to 400 kV (SvK, 2024). The purpose of the transmission grid is to transport large amounts of electricity long distances with minimal losses. Distribution grids are connected to substations within the transmission grid, which then distribute electricity to consumers. Some large electricity producers and customers are also connected directly to the transmission grid (SvK, 2024). Regional grids connect cities and regions to the transmission grid and are the first part of the distribution grid. The regional grid operates with a voltage between 42 kV and 152 kV, and more producers and consumers can be connected to the regional grid. The last type of grid is the local grid, which connects the rest of the producers and consumers to the power system. Local grids have a voltage level from 400 V and up to 40 kV (Energimarknadsinspektionen, 2024).

To streamline the terminology used throughout this report, standards according to IEC 50160 will be introduced. The local grid will be defined as low voltage (LV) and medium voltage (MV) grids, regional grid as high voltage (HV) grid, and the transmission grid as extra high voltage (EHV) grid. A summary of this will be presented in Table 1. Note that the voltage levels are not completely the same as those from Energimarknadsinspektionen (EI) mentioned above, but it will not make any difference in this report.

Table 1 - Definition of voltage levels used in IEC 50160 (IEC, 2022). U_n is the nominal system voltage.

Voltage level	Voltage
Low voltage, LV	$U_n \leq 1\ kV$
Medium voltage, MV	$1\ kV \leq U_n \leq 36\ kV$
High voltage, HV	$36\ kV \leq U_n \leq 150\ kV$
Extra high voltage, EHV	$150\ kV \leq U_n \leq 800\ kV$

2.1.2 Electricity production

During 2024, hydropower produced the largest share of electricity in Sweden, with about 40% of the total of 162 TWh. The second largest source was nuclear closely followed by wind with 30% respectively 25% of the total production (SvK, 2025). Sweden's energy production is expected to double in the next 25 years, with wind and solar making up a significant portion (Energimyndigheten, 2023). Wind and solar power sources cannot, in most cases, be connected directly to the electrical grid. This is because they generate either direct current (DC) voltage or alternating current (AC) voltage with variable frequency and voltage, which is not compatible with the grid's standard of 50 Hz AC. To enable grid integration, frequency converters are required. These frequency converters transform the variable frequency AC or DC output into the correct AC voltage at 50 Hz, ensuring compatibility with the grid. (Kroposki, 2024).

2.2 HYDROPOWER PLANT

A hydropower plant (HPP) converts the kinetic energy of flowing water into electricity, which then is fed into the grid. HPPs vary in size, from a few kilovolt-ampere (kVA) in so-called micro-HPPs to several hundred megavolt-ampere (MVA) in the larger ones, but the operating principle is the same regardless of size. Electricity generation at HPPs requires a combination of water flow and pressure. The water flow is naturally provided by our rivers, and the pressure is created by the height difference between the upstream and downstream water levels, which can be improved with a dam. This pressurized water drives a turbine, which then is connected to a generator. At this step, the kinetic energy of the water is converted into electrical energy (EIA, 2023).

As the generator rotates, a magnetic field associated with the rotational motion induces a voltage in the stator windings, which in turn causes a current to flow if the circuit is closed. This current is then fed through cables to the next major equipment, the transformer. A transformer is the link between the generator and the grid since it converts the relatively low voltage and high current produced by the generator into a higher voltage and lower current. Together, the generator and transformer enable the conversion of the turbine's rotational kinetic energy into electrical energy that can be delivered through the grid and used by consumers. A HPP does also require other auxiliary equipment to ensure safe and reliable operations.

Accurate measurements of current and voltage are essential for monitoring power output and detecting potential faults. If a fault occurs, it is critical to be able to disconnect equipment to prevent damage. The measurements are generally conducted with measurement transformers, and the disconnections are carried out using circuit breakers. This equipment will be further explained in this section.

2.2.1 Generators

A generator converts rotating kinetic energy into electric energy. The fundamental principle of a generator is based on Faraday's law of electromagnetic induction, where a varying magnetic field induces a voltage in a conductor. In a HPP, there are two types of generators commonly used, synchronous and asynchronous, with the synchronous type being the most common. The primary difference between these two lies in how the magnetic field in the rotor is produced, while both have a similar stator design. The stator is the stationary part of the generator where the voltage is induced by the magnetic field in the rotor. A stator has loops of conductors placed and connected in a specific way, commonly referred to as windings. Depending on how these windings are placed and connected, the machine will have different properties. The windings from the stator are then connected to the electric grid, which creates a rotating magnetic field in the stator (Wildi, 1991).

In a synchronous generator, the rotor rotates at the same speed as the magnetic field in the stator. The magnetic field in the rotor is produced by field windings mounted on the rotor, which are supplied with a DC current. In an asynchronous generator, the rotor does not rotate at the same speed as the stator field, and the current for magnetizing the rotor is induced by the magnetic field in the stator. The difference between the rotational speed of the rotor and magnetic field in the stator is referred to as slip (Wildi, 1991).

2.2.2 Transformers

Transformers are used to connect two different voltage levels. An oscillating voltage in a coil produces a varying magnetic flux that in turn induces a voltage in a different coil. By adjusting the number of turns in each coil, the transformer can increase or decrease the voltage level. For an ideal transformer, this can be described with Equation 1 where U is the voltage in volts, I is the current in ampere, N is the number of turns in the coil and a is the ratio value. The subscripts *1* and *2* refer to primary and secondary sides of the transformer (Wildi, 1991).

$$\frac{U_1}{U_2} = \frac{I_2}{I_1} = \frac{N_1}{N_2} = a \tag{1}$$

To enhance efficiency, the coils are wound around an iron core, as iron conducts magnetic flux more effectively than air. How well a material conducts magnetic flux depends on the permeability of the material. For example, air has a permeability around *one* while iron can have a permeability in the range of several thousand, making it thousands of times better than air to conduct magnetic flux. However, the permeability of a material will change depending on how much magnetic flux is flowing through it. At some point, no more flux will be able to flow, and the material will be saturated. Before the point of saturation, the knee point, the material is relatively linear, meaning that an increase in electric voltage in the primary coil will give an equally large difference in the magnetic flux. After the knee point, increasing the voltage on the primary coil will not induce more magnetic flux (Wildi, 1991). A simplified

explanation of this can be seen in Figure 1 where Equation 1 holds reasonably well until the material gets saturated at the knee point.

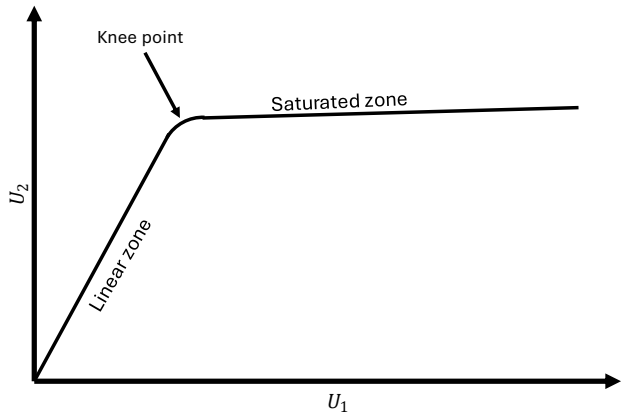

Figure 1 - Illustration of the knee point in a voltage transformer. Below the knee point, an increase of the applied voltage to the primary coil results in a proportional increase in the secondary voltage with a ratio of U_1/U_2. After the knee-point, no significant increase over the secondary coil occurs even if the primary voltage increases.

There are two main types of transformers that are used at a HPP, measurement transformers and power transformers.

2.2.2.1 Power transformers

Power transformers are used to connect different voltage levels to each other. The rated voltage and power depend on the type, with the largest units capable of transferring several hundred MVA at voltage levels of several hundred kV. Three-phase transformers are commonly used in the power system, and the three phases can be connected in different configurations. A *delta*-connected transformer will have three terminals with the phase-to-phase voltage between each terminal, and a *wye*-connected transformer can have four terminals, one for each phase and one connection to the neutral point. The secondary side windings in distribution transformers are typically connected in a *wye* configuration to enable access to the phase to neutral voltage. A distribution transformer can be explained as the type of transformer connecting LV grids with MV grids (Wildi, 1991). The choice of winding configuration influences how the transformer responds to harmonic components, which will be discussed in Section 2.3.1.1. To optimize material usage, power transformers are designed to operate with a flux density just below the knee point under rated load conditions. One of the key aspects of the design of a power transformer is high efficiency, which generally is above 95% (Glover, Overbye and Sarma, 2017).

2.2.2.2 Measurement transformers

Since measurements cannot be performed directly on high voltage levels, measurement transformers are used to scale down the high levels to measurable levels. While these devices measure either current or voltage, they share the common operating principle according to Equation 1. In this case, high accuracy is more important than efficiency unlike in power transformers where efficiency often is prioritized (Wildi, 1991).

To ensure the same accuracy for different measurement transformers, standardized accuracy classes have been established. The accuracy class of a measurement transformer is expressed

as a percentage of how large the error is allowed to be. Each value also comes with a maximum allowed phase displacement error. There are different accuracy classes depending on the purpose of the measurement. Metering measurements allow lower error margins, whereas protective measurements permit higher errors but must withstand extreme fault conditions. One drawback with these classes is that they are only valid for frequencies around the fundamental frequency and not for harmonics (ABB, 2015). For example, an accuracy class of 0.1 in a voltage transformer means that the maximum permissible error is $\pm 0.1\%$ of the actual voltage, along with maximum phase angle error, both within a predefined voltage range around the rated voltage. The burden connected to the secondary winding must also be appropriate. Burden refers to the load connected to the secondary winding of the transformer. It is typically expressed in VA (volt-amperes) and represents the total power drawn by connected devices such as meters, relays, or other instrumentation (ABB, 2015). However, the burden can also be expressed in terms of impedance, provided the voltage and power are known.

Measurement transformers can either be designed for metering purposes or protective purposes. Measurement transformers for measuring purposes are designed to saturate their iron core at a lower level to protect the connected measurement equipment from high voltages and currents. In contrast, measurement transformers for protective purposes are designed to handle higher levels to allow for functionality during fault conditions. (Elfving, 1993; ABB, 2015).

2.2.3 Cable systems

Cables are used to connect equipment within the HPP and can also be used in the electrical grid where overhead lines are not suitable. A cable is a conductor with an insulating layer around it, eliminating the need for separation required for insulation in an overhead line. The design of the cable differs between voltage levels. However, this thesis focuses on MV cables, which are common in HPPs.

2.2.3.1 Cables

A MV cable is composed of several layers which will be presented in this section. A conductor is located in the core of the cable, typically made of copper or aluminum. Around the conductor is a thin semi-conducting layer applied to smooth out any uneven parts of the conductor, minimizing the risk of sharp edges that can cause high electric fields. Next, insulation is added to handle high electric fields. A second semi-conducting layer is then applied around the insulation before the metallic shield, which will have ground potential, is applied. All these parts are illustrated in Figure 2 below. This is the main part of the cable in order to handle the electric field. There are often more layers outside this to protect the cable from physical damage (Worzyk, 2009).

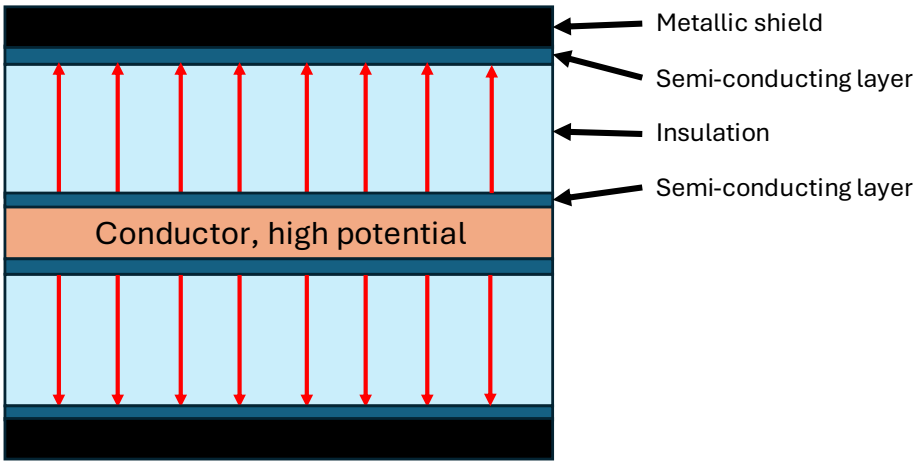

Figure 2 - Parts of a MV cable essential for handling the electric field. Red arrows indicate how the electric field points from the conductor towards the grounded shield.

2.2.3.2 Cable termination

When a cable needs to be connected to equipment or any accessory, it is necessary to cut the cable and remove a portion of the metallic shield and semi-conducting layer. This will cause a high electric field at the edge of the semi-conductive layer according to Figure 3. This field will cause dielectric stress in the insulation material, which will result in a breakdown of the cable (IEEE, 2021).

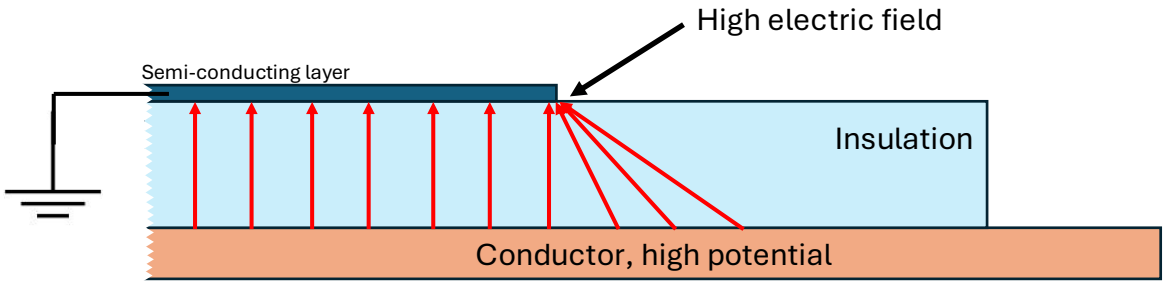

Figure 3 – End of a cable without a cable termination. High electric fields will occur where the semi-conductive layer ends. The red field lines are for illustrative purposes, and their paths have therefore been simplified.

To address the issue of high electric fields, cable terminations are used to control the field. There are a few different types of cable terminations available with various properties. However, for MV applications, non-geometric designs with a resistive/refractive stress grading layer are common due to their simplicity and slim design. The stress grading layer has resistive properties which evens out the electric field over the length of the stress grading layer, resulting in a lower maximum electric field. Figure 4 shows where the stress grading layer is applied. Due to the resistive properties of the stress grading material, some heat losses will occur in the material (Paulsson et al., 2003).

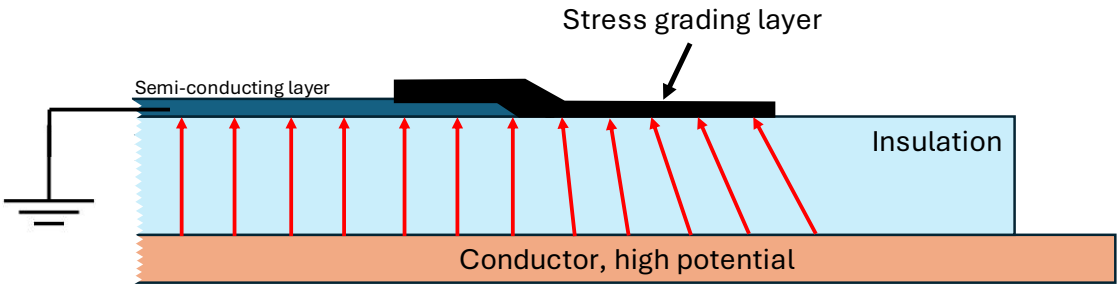

Figure 4 - Cable termination with a stress grading layer. The electric field is in this case spread out over a longer distance, thereby reducing the maximum electric field strength.

2.2.4 Relay protection

Protecting all equipment within a HPP is essential. For this reason, protective relays are used. The definition of a protective relay is according to IEEE (1992): "*A relay whose function is to detect defective lines or apparatus or other power system conditions of an abnormal or dangerous nature and to initiate appropriate control circuit action*." There are numerous different types of protective relays at a HPP, but a generalized description of how they work is that they use a signal from a sensor and if any abnormalities are detected a breaker disconnects the fault (Wildi, 1991).

2.3 HARMONICS

There are many power quality issues that can cause problems in the power system. This thesis will, however, only focus on harmonics. In this section, an explanation will be provided of what harmonics, interharmonics and supraharmonics are. An overview of how harmonics in the grid are created, how large they can be according to standards, and a simplified model on how they can propagate in a grid will be presented.

2.3.1 Types of harmonics

Harmonic frequencies can be divided into several subcategories based on their frequency. Three of these relevant for this thesis are presented below.

2.3.1.1 Harmonics of the fundamental frequency

Harmonics are multiples of a fundamental frequency. The fundamental frequency in the electrical grid is 50 Hz or 60 Hz. In this thesis, the fundamental frequency is defined as 50 Hz, meaning that the alternating voltage and current oscillate 50 times each second. All harmonics are frequencies that, when divided by the fundamental frequency, result in a positive integer (IEC, 2022). For example, the second harmonic will have a frequency of 100 Hz, the third 150 Hz, the fourth 200 Hz and so on. Harmonics are superimposed onto the fundamental frequency, creating a resulting waveform. An example of this can be seen in Figure 5, where the fifth harmonic with an amplitude of 0.1 units have been superimposed onto the fundamental frequency with the amplitude of one unit generating a resulting waveform. All power grid operators strive to have only the fundamental frequency in the grid, but there will always be harmonics with different amplitudes in the grid.

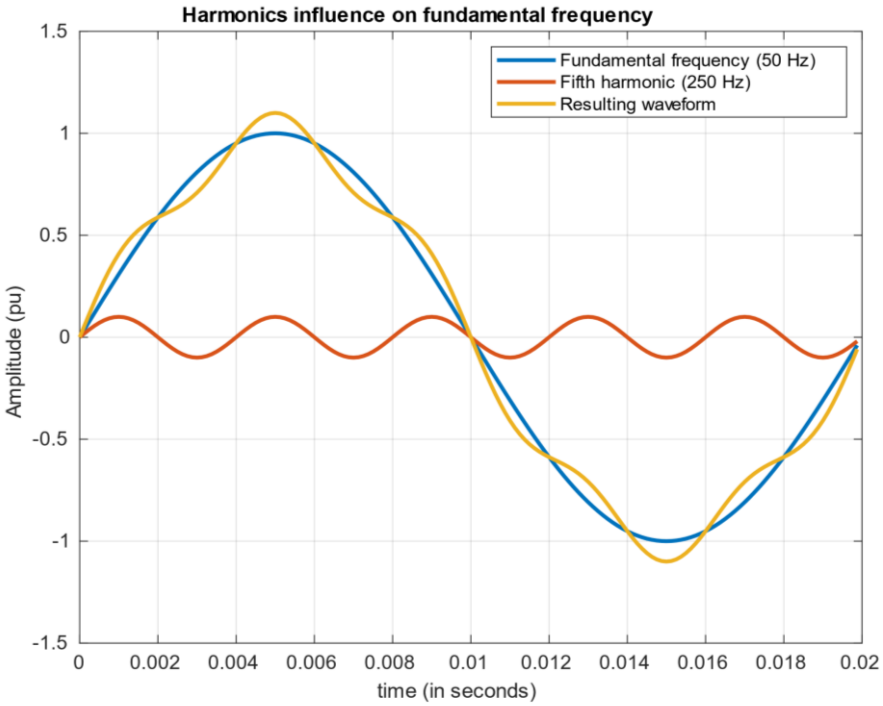

Figure 5 – The fifth harmonic (red) is superimposed on the fundamental frequency of 50 Hz (blue), generating a resulting waveform (yellow).

Phase sequence of harmonics

Table 2 shows the phase sequences of the ten first harmonics. The same patterns repeat for higher-order harmonics. To understand the phase sequences, an example with a three-phase electric motor can be used. Positive sequence harmonics produce a rotating field in the same direction as the fundamental frequency; negative sequence will cause a rotation in the opposite direction, and the negative does not cause any rotation. However, all of the sequences will generate heat losses (Gustavsson, 2003).

Table 2 - Phase sequence of the ten first harmonics.

Order	1	2	3	4	5	6	7	8	9	10
Frequency (Hz)	50	100	150	200	250	300	350	400	450	500
Sequence	+	-	0	+	-	0	+	-	0	+

Harmonics in the power system

Even harmonics in the power system tend to be small, as few sources generate even harmonics. They also tend to cancel each other out due to symmetry (Gustavsson, 2003). Zero-sequence harmonics cannot enter or leave a delta winding in a transformer and are therefore stopped in transformers. Wye connected windings without a high impedance between the neutral point to ground will also limit zero-sequence harmonics (Glover et al., 2017). This leaves only the odd harmonics that are not divisible by three, which will be referred to as characteristic harmonics in this thesis.

2.3.1.2 Interharmonics

Interharmonics is a sinusoidal voltage or current waveform with a non-integer multiple of the fundamental frequency. They may appear as individual frequencies or as a wide band spectrum (IEC, 2022). Interharmonics has traditionally not been an issue in the grid to a large extent since most of the connected equipment is synchronized to the fundamental frequency and thus primarily generates multiples of that. Interharmonics is most commonly generated in two ways. The first, rapid non-periodic changes, which for example could occur during transients. The second, and the primary source considered in this thesis, is the switching of frequency converters that are not synchronized with the system frequency (Marz, n.d.).

All harmonics, including interharmonics, can be described by phasors with associated phase sequences. However, the phase sequences for interharmonics are more complex, as any given interharmonic can be a combination of both positive and negative sequence components (Zhang, Xu and Liu, 2005).

2.3.1.3 Supraharmonics

Supraharmonics are harmonics with a frequency between 2 kHz and 150 kHz and mainly generated by power electronics with high switching frequencies. This will be further discussed in Section 3.

2.3.2 Sources of harmonics

Harmonics is primarily caused by non-linear equipment in the power grid. Non-linear equipment draws a current that is not proportional to the applied voltage (Gustavsson, 2003). Figure 6 illustrates an example of a distorted current waveform together with its frequency spectrum caused by a single-phase non-linear load. The power system contains numerous non-linear sources and loads. However, as this thesis does not aim to identify the origin and creation process of each measured harmonic, only a selection of relevant sources will be presented below.

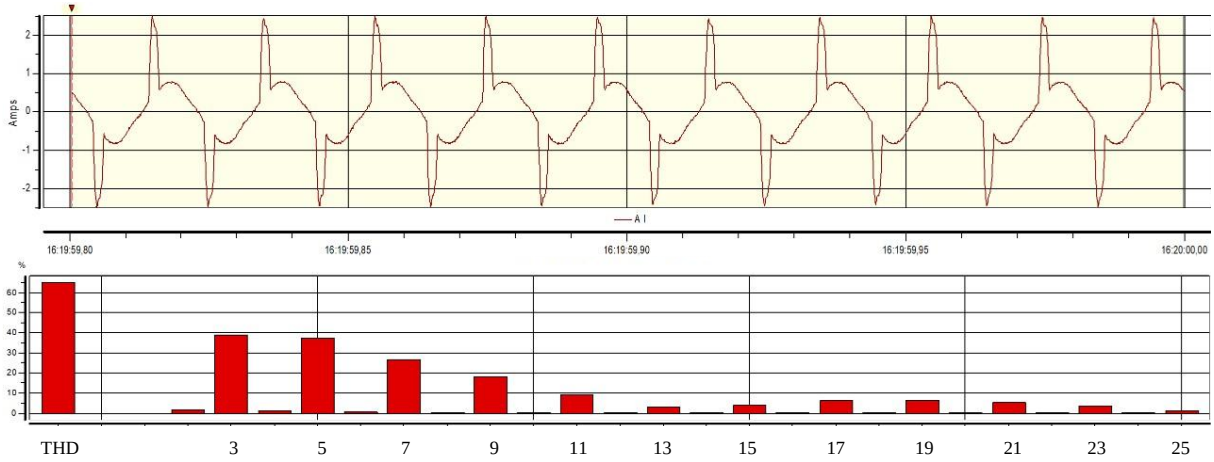

Figure 6 - Example of distorted current waveform and frequency spectrum. Note that no even harmonics are present, but triple harmonics are present since a single-phase load was measured.

2.3.2.1 Frequency converters

A frequency converter can be described as a rectifier, a DC stage followed by an inverter, as illustrated in Figure 7. With a frequency converter, a signal with one frequency can be converted into a signal with a different frequency. This could, for example, be used to connect a variable speed wind turbine to the grid or to connect motors that need a variable frequency to control the speed. In some cases, it can be beneficial to only use the rectifier or inverter stage if a DC voltage is present, such as in a battery energy storage system. The switching can be performed using insulated-gate bipolar transistor (IGBT) together with pulse width modulation (PWM) techniques (Yang et al., 2014). Since the IGBTs can be switched on and off independently of the grid frequency, harmonics can be generated at all frequencies including interharmonics (Marz, n.d.).

Figure 7 - Stages of a frequency converter. If a DC signal is required, only the rectifier or inverter should be used. Figure inspired by (Thunberg, 2001).

Switching of the IGBTs is controlled by the PWM signals, which consists of a carrier wave and a reference wave. The frequency of the carrier wave determents the switching frequency of the IGBTs. Since switching frequency is a commonly used term to describe this, it will therefore also be used in this report. In three-phase frequency converters, harmonics can be generated around integer multiples of the switching frequency according to Equation 2. f_h is the frequency of the harmonic component, N is an integer and f_s is the switching frequency. As N increases, the amplitude of the harmonics decreases (Analog Devices, n.d.). Figure 8 illustrates a simplified representation of the harmonics generated by PWM switching.

$$f_h = Nf_s \tag{2}$$

As an example, when Equation 2 is used with a switching frequency of 3 kHz, harmonics will appear around frequencies 3, 6, 9, 12, … kHz, and so on. The amplitudes are, however, decreasing at higher frequencies.

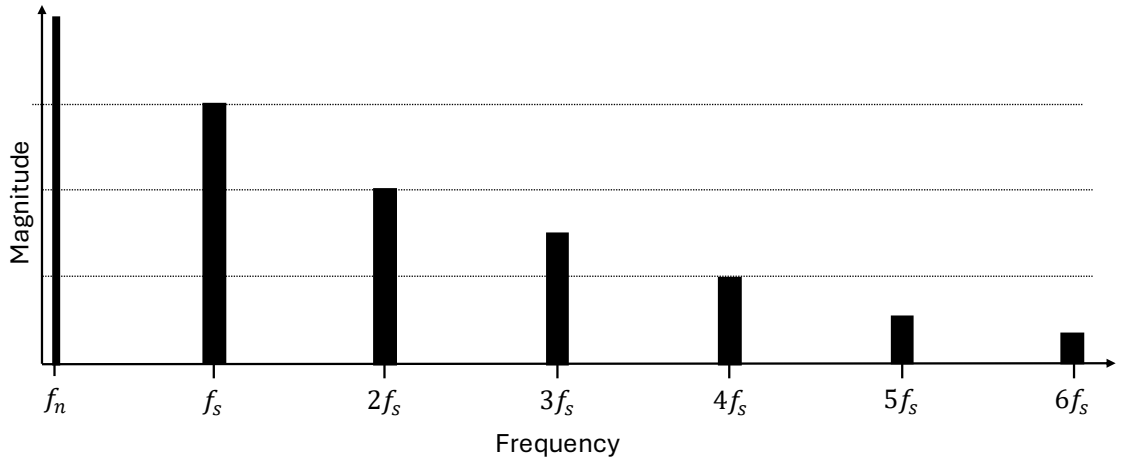

Figure 8 - Harmonic frequencies due to PWM switching in three phase converters. f_s is the switching frequency and f_n is the nominal system frequency.

2.3.2.2 Wind power

Modern wind turbines use a frequency converter to connect to the grid. This enables the turbine to rotate at variable speeds to maximize efficiency at each wind speed. The switching is generally performed with IGBTs with a variable switching frequency (Yang et al., 2014). Two common types of turbines discussed in this thesis are the permanent magnet synchronous generator (PMSG) and the double fed induction generator (DFIG).

The PMSG is a variable-speed turbine that has a full frequency converter, hence all power generated from the turbine will pass through the converter. This type can generate both harmonic and interharmonic current emissions, including characteristic harmonics and switching-related supraharmonics, as described by Equation 2 (Behkesh Noshahr, 2016).

A DFIG is a variant of an asynchronous generator in which the stator windings are directly connected to the grid. The main difference between the two is that the DFIG has field windings for excitation, which are fed by AC current generated by a frequency converter. This configuration allows for variable-speed operations, as the frequency converter that can control the frequency of the current supplied to the rotor. In this type, only a portion of the total generated power passes through the frequency converter, while the majority passes through the grid-connected stator windings (Breeze, 2016).

Harmonic emissions can vary depending on both the type and wind speed. Yang et al. (2014) performed measurements of current harmonic emissions from three different wind turbines. The first turbine is a DFIG generator with a rated power of 2.5 MW and six poles in the rotor. The second is also a DFIG turbine but with a rated power of 2 MW and four poles. And the third turbine is a PMSG with a full frequency converter. The study measured harmonic emissions at various levels of power production. Key findings from this analysis relevant to this thesis are summarized below:

- The spectrum contains both narrow band and broadband components for all turbines.
- Large interharmonics were observed.
- Even harmonics and interharmonics had a relatively high amplitude.

- Interharmonics showed a strong dependency on active power production. They were highest when power production was at its peak and lowest when production was at its lowest.

2.3.2.3 Iron cores

Harmonics can be generated by saturation in iron cores due to the non-linearity of the material explained in 2.2.2. (Thunberg, 2001). For instance, if the iron core of a transformer becomes saturated as explained in 2.2.2, the secondary voltage waveform can be distorted compared with the primary voltage.

2.3.2.4 Hydropower plants

HPPs can generate harmonic emissions, for example, in the generator. However, these harmonics are well understood and can therefore be minimized in the design of the generator (Wakileh, 2003). Ashrafpour and Shahgholian (2020) have compared the harmonic emissions generated by HPPs and wind farms and their impact on the power system. One of the conclusions from the study was that harmonic distortion caused by HPPs can be neglected in a power system compared to the distortion from wind farms. However, the impedance of the HPP will have an impact on the harmonics of the total system.

2.3.3 Harmonic propagation in the grid

The propagation of harmonics in grids depends on a variety of factors, which will not be discussed in detail in this thesis. A simplified explanation can be made using ohms law. Consider a transmission line connecting point A with point B. At point A, a harmonic source emits a harmonic current with frequency f, and at point B, the voltage harmonic with frequency f is measured. The frequency dependent impedance between the two points is Z_f and the voltage at point B can therefore be calculated with Equation 3 (Ashrafpour and Shahgholian, 2020).

$$U_f = Z_f I_f \tag{3}$$

The impedance Z_f can vary significantly with frequency due to resonance phenomena and other loads in the system. An example of this frequency-dependent grid impedance is illustrated in Figure 9 by Ashrafpour and Shahgholian (2020). Other harmonic sources might inject harmonic currents from other locations, and the grid is often meshed, making the system even more complex.

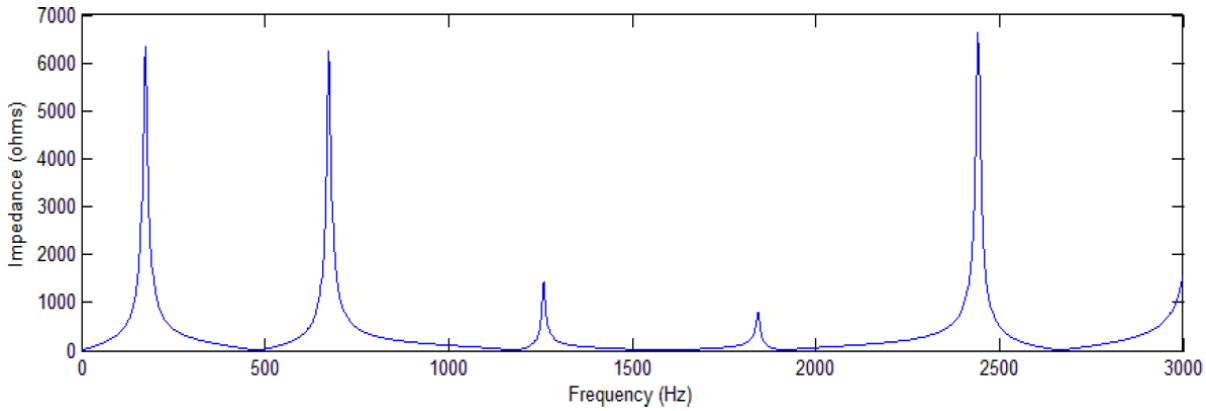

Figure 9 - Example of grid impedance for different frequencies. Source: (Ashrafpour and Shahgholian, 2020)

2.3.4 Standards for voltage harmonics in the electrical grid

IEC 50160 is an international standard that defines the voltage characteristics of electricity supplied by public distribution networks (IEC, 2022). This standard includes, among other things, definitions of allowed levels of voltage harmonics at different voltage levels. According to the standard, during a one-week period, 95% of all 10-minute average RMS values must remain below the specified maximum for each voltage level. The measurement procedure for this is defined in other standards, explained in Section 4.2.1. A list of allowed individual harmonics can be found in Appendix B, but relevant values will also be presented in the results. The total harmonic distortion of voltage for HV and EHV grids is under consideration in the IEC 50160 standard. These values will instead be collected from the IEEE 519 standard (IEEE, 2022). No levels of interharmonics have been presented in the IEC 50160 standard, but those are under review pending further experience.

2.3.4.1 Total harmonic distortion

The total levels of harmonics in a signal can be described with the total harmonic distortion (THD). This value can be calculated with Equation 4 where G_n is the amplitude of the voltage or current harmonic component and G_1 is the fundamental voltage or current (IEC, 2002). H is the highest harmonic order considered in the analysis. According to IEC, (2022), harmonics up to the 40th order should be evaluated when calculating the THD.

$$THD = \sqrt{\sum_{n=2}^{H} \left(\frac{G_n}{G_1}\right)^2} \tag{4}$$

There is also a connection between the RMS values of a signal and the THD. The RMS value of a signal containing harmonics can be calculated with Equation 5.

$$G_{rms} = G_1\sqrt{1 + THD^2} \tag{5}$$

2.4 CIRCUIT THEORY

This section provides a brief overview of circuit theory, which will be used in the following sections.

2.4.1 Real and imaginary

In circuit analysis, voltage, current and impedance can be described with imaginary numbers. A purely resistive load has only a positive real part, a purely inductive load has only a positive imaginary part, and a purely capacitive load has only a negative imaginary part.

2.4.1.1 Resistance

Resistance describes how easily a current can flow through a conductor. It is measured in *ohms* and is a real quantity without phase shift. The easiest way of defining resistance of a conductor is to define the DC resistance, which is given in Equation 6, where l is the length of the conductor in meters, σ is the conductivity of the material and A is the cross-sectional area of the conductor. (Glover et al., 2017).

$$R_{DC} = \frac{l}{\sigma A} \tag{6}$$

To only use the DC resistance when using AC, especially at high frequency harmonics, would be wrong since the AC resistance is larger than DC resistance. AC resistance could be calculated with frequency dependent parameters with Equation 7 (Novitskiy, Schlegel and Westermann, 2020).

$$R_{AC} = R_{DC}\left(1 + \gamma_S + \gamma_p + \gamma_{SC}\right) \tag{7}$$

γ_S is the factor for the frequency dependent skin effect which makes the useful conductor area in a conductor smaller, increasing the resistance. γ_p is a factor for the frequency dependent proximity effects where nearby currents push each other away from each other due to their magnetic fields and limiting the useful conductor area. γ_{SC} is a factor that takes the screen of a cable into consideration if it is a cable. These terms are not easy to use in practical applications without simulation software due to the complexity of the geometry. Equations for each term can be found in the standard IEC 60287-1-1 (Novitskiy et al., 2020).

2.4.1.2 Capacitance

Capacitance is a fundamental electrical property that describes an object's ability to store electric charge and has the unit *farad* (Boylestad, 2016). Stray capacitance, also known as parasitic capacitance, is unwanted capacitances that do exist in all equipment where two different potentials are present. Stray capacitances can be found in, for example, a transformer, such as the capacitance between the primary winding and ground, secondary winding and ground and primary winding to secondary winding (Liu et al., 2018). Cables are also a source of capacitance in the power system (Worzyk, 2009).

Capacitive reactance is a frequency dependent quantity defined in Equation 8 where f is the frequency in *hertz* and C is the capacitance (Boylestad, 2016).

$$X_C = \frac{-j}{2\pi f C} \tag{8}$$

2.4.1.3 Inductance

Inductance is a fundamental electrical property that describes the opposition to change in current flow and has the unit *henry*. Coils, including the winding coils found in transformers, commonly possess inductances in power systems.

Inductive reactance is a frequency dependent quantity defined in Equation 9 where f is the frequency in *hertz* and L is the inductance in *henry* (Boylestad, 2016).

$$X_L = j2\pi fL \tag{9}$$

2.4.1.4 Impedance

Impedance is the opposition to current flow when an AC circuit contains a combination of resistance, capacitance, and inductance. Impedance is defined in the complex plane with the circuit elements as vectors and have the unit *ohm*. Impedance can be written in a cartesian form as in Equation 10 (Boylestad, 2016).

$$\mathrm{Z} = R + (X_L + X_C) \tag{10}$$

2.4.2 Resonance

Resonance in a power system can occur when the frequency of a signal matches a specific combination of capacitance and inductance in the system. Resonance can take place in two different ways, series and parallel resonance. The frequency at which the first resonance occurs, f_0, can be calculated with Equation 11 (Gustavsson, 2003).

$$f_0 = \frac{1}{2\pi\sqrt{LC}} \tag{11}$$

2.4.2.1 Series resonance

Series resonance occurs when the inductance and capacitance are aligned in series. X_L and X_C will at frequency f_0 have the same absolute value but with a phase shift of 180°. This results in a cancellation of the complex part of the impedance, leading to a minimum impedance with a phase angle of zero degrees. In this situation resistance is the only thing limiting the current flow (Boylestad, 2016). An example of a series resonance circuit with a resonance frequency of 2 kHz is illustrated in Figure 10. The resonance frequency is calculated with Equation 11.

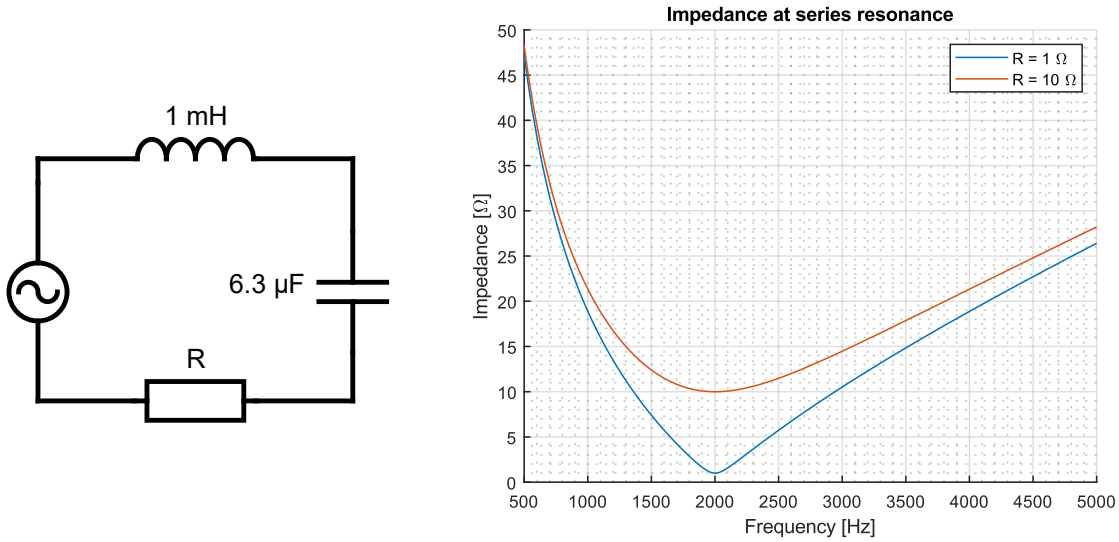

Figure 10 – An example of a series resonance circuit with a resonance frequency of 2 kHz. The plot to the right shows the impedance seen by the source at various frequencies. The lowest impedance can be found at the resonance frequency of 2 kHz.

2.4.2.2 Parallel resonance

Parallel resonance occurs when the capacitance and inductance are aligned in parallel. When the harmonic frequency in this scenario fulfills Equation 11, a point of maximum impedance is found. This could generate high voltages even at a low current according to Equation 3 (Eghtedarpour, Karimi and Tavakoli, 2014). An example of a parallel resonance circuit with a resonance frequency of 2 kHz is illustrated in Figure 11. The resonance frequency is calculated with Equation 11.

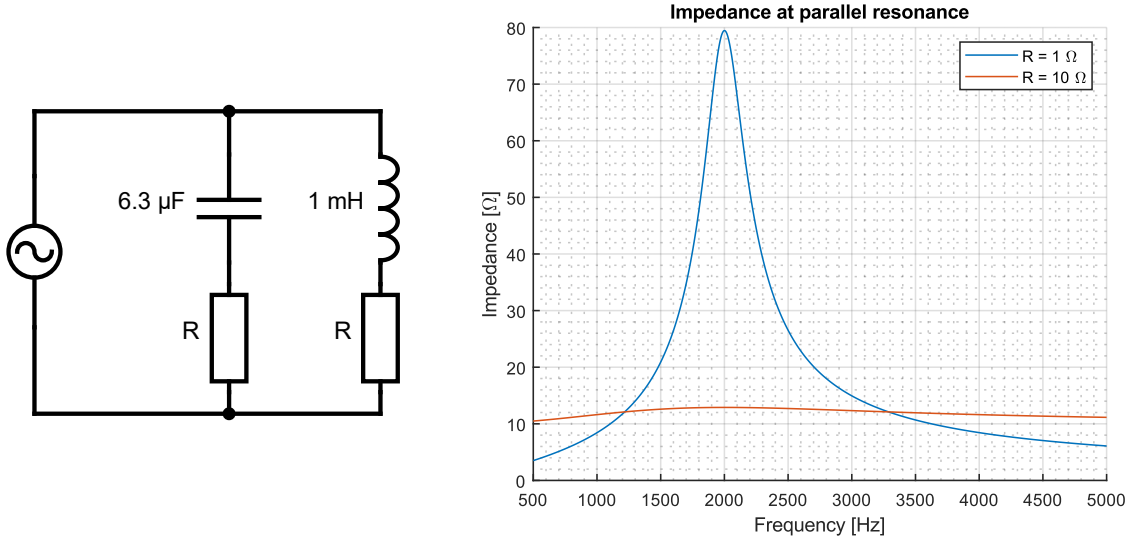

Figure 11 - An example of a parallel resonance circuit with a resonance frequency of 2 kHz. The plot to the right shows the impedance seen by the source at various frequencies. The highest impedance can be found at the resonance frequency of 2 kHz.

2.4.3 Losses in the power system

There are many types of losses in the power system, and this section will describe some of the most relevant for this thesis. All of these losses are frequence-dependent, meaning that harmonics can cause significant losses even at small magnitudes.

2.4.3.1 Copper losses

Copper losses are caused by the current flowing through a conductor and are frequency dependent. Copper losses can be calculated with Equation 12, where P_{cu} is active power loss in *watts*, $I_{RMS,h}$ is the RMS current for the harmonic component with order h and $R_{AC,h}$ is the resistance for the harmonic component of order h, defined in Equation 7. Equation 12 is derived from Ghorbani and Mokhtari, (2015), and the AC resistance in Equation 7.

$$P_{cu} = {I^2}_{DC} R_{DC} + \sum_{h=1}^{h=h_{max}} {I_{RMS,h}}^2 R_{AC,h} \tag{12}$$

2.4.3.2 Eddy current losses

Eddy current losses occur when circulating current is induced into the iron core of electrical machines, such as transformers and generators, and are also frequency dependent. Eddy current losses can be calculated with Equation 13. K is a proportionality constant, B is the flux density, f is the frequency, d is the material thickness, and ρ is the resistivity (Shokrollahi and Janghorban, 2007).

$$P_e = \frac{KB^2 f^2 d^2}{\rho} \tag{13}$$

2.4.3.3 Dielectric losses

Dielectric loss occurs in insulating materials, such as insulation in cables, generator coils, or the insulating oil in a transformer. Dielectric losses may occur in an insulating (dielectric) material when two electric potentials are separated by the dielectric material. An ideal insulation will be purely capacitive with no resistive component, hence not cause any active power loss. In real materials, resistive components may be present due to the material's properties and imperfections, leading to active power loss and heating. The dissipation factor or $\tan(\delta)$ is a measure of how resistive or capacitive a material is and can be calculated with Equation 14. With this, the dielectric power loss can then be calculated using Equation 15. I_R is the resistive current and I_C is the capacitive current (Worzyk, 2009).

Over time, the resistive current may increase due to material aging, which in turn elevates heat losses and further accelerates the aging process. This degradation can be intensified by additional heat generated from voltage harmonics. (Akin and Arikan, 2023).

$$\tan(\delta) = \frac{|I_R|}{|I_C|} \tag{14}$$

$$P_d = C \tan(\delta)\, 2\pi f U^2 \tag{15}$$

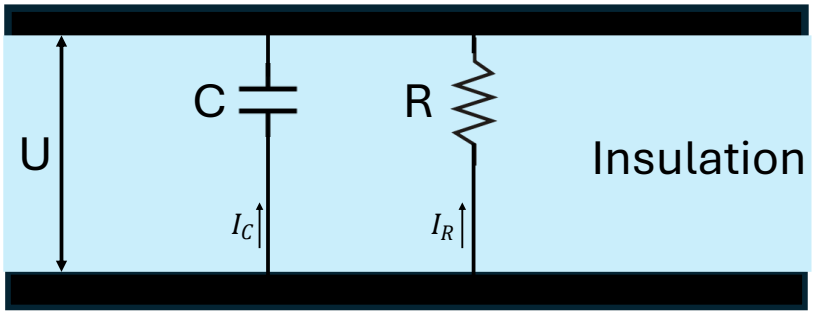

Figure 12 - Model of an insulating material between two different potentials with a difference of U volts. Losses are generated in the resistive part from the resistive current I_R.

2.5 MEASUREMENT TECHNIQUES

To accurately measure harmonics in the power system, a measuring system is required. The general principle is similar between voltage and current measurements. Focus will however be on the voltage measurements in this thesis. A schematic of the measuring system is presented in Figure 13 and is a summary of instructions found in IEC 61000-4-7 (IEC, 2002).

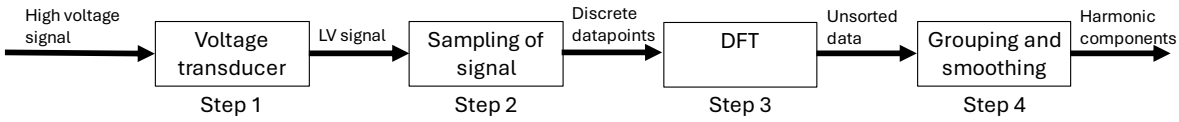

Figure 13 – Overview of the procedure for measuring voltage harmonics at higher voltage levels according to the standard IEC 61000-4-7.

Step one outlined in Figure 13 is to convert the high voltage signal into a safe low voltage signal. This can be achieved with a measurement transformer or a voltage divider. Normal measurement transformers can introduce significant errors in both amplitude and phase angle, which is further described later in this section. In this thesis, the measurement uncertainties of this step represent the largest source of measurement error.

Step two in the process is to sample the analog voltage signal to a digital signal. This requires a high enough sampling rate together with a high resolution for accurate measurement. The sampling frequency must however be at least twice as high as the highest frequency component in the signal to be able to recreate a good representation according to the Nyquist theorem (Austerlitz, 2003).

The two last steps are where the digital signal is processed to give useful information. This is achieved using the discrete Fourier transform (DFT) that builds on the Fast Fourier transform (FFT) algorithm. All periodic waveforms can be represented as a sum of sinusoidal waveforms according to the Fourier series theorem. The FFT is an algorithm that can be used to calculate the amplitude and frequency of each individual sinusoidal waveform. Digital power quality analyzers typically use the FFT algorithm to compute the DFT of the sampled signal. (IEC, 2002).

This thesis will focus on the first step and not go into details of the digital parts described in the later stages. It is important to remember that measurement errors can occur with a poorly chosen measurement instrument (Artale et al., 2022).

2.5.1 Measurement transformers

Normally, voltage and current at higher voltage levels are measured using measurement transformers. Many of these are not suited for harmonic measurements due to their limited frequency range. This section presents the common measurement transformers used in high-voltage applications.

2.5.1.1 Inductive voltage transformer

An inductive voltage transformer (IVT) works on the principle of induction. Equation 1 is valid for an ideal transformer during no load conditions. In reality, a voltage drop will occur in the windings due to resistance and leakage reactance which needs to be taken into consideration when designing the measurement system (ABB, 2015).

IVTs are designed for an operating frequency where accuracy is defined. Outside this frequency, large ratio errors and phase angle errors can occur. These errors are primarily caused by resonance effects between the core inductance and the capacitance of the primary windings. At resonance frequencies, either a peak or a trough can be seen in the error. The first resonance point is a peak if a parallel resonance occurs and a trough if a series resonance occurs (Douglass, 1981). Meyer et al., (2011) conducted frequency response measurements of approximately 100 IVTs from 50 Hz up to 5 kHz. Some of the key findings were that the frequency up to which accurate measurements of harmonics generally are possible decreases with higher voltage levels. An example of frequency responses for different voltage levels is illustrated in Figure 14. The frequency up to which a measurement with acceptable accuracy can be performed is mentioned as the critical frequency. The critical frequency is always located below the first resonance point and will vary depending on different thresholds for accuracy. Figure 15 shows an illustration of the critical frequency at different accuracy thresholds. Not only does the rated voltage have an impact on the critical frequency, but the specific design of the IVT among other things also plays a significant role.

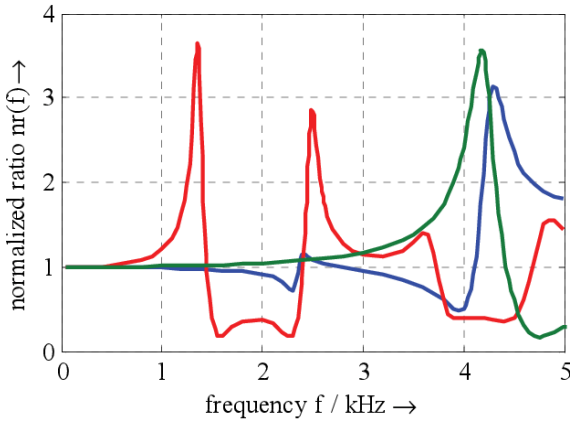

Figure 14 - Example of errors for different IVTs and voltage levels, 66 kV (green) 110 kV (blue) and 220 kV (red). Source: (Meyer et al., 2011)

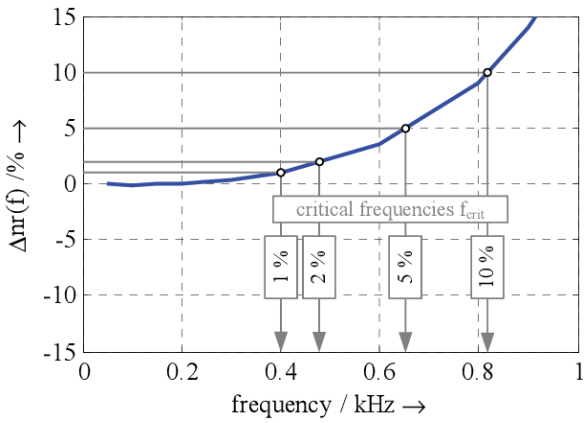

Figure 15 - Example of critical frequencies at different accuracy thresholds. Source: (Meyer et al., 2011)

The findings from Meyer et al. (2011) served as the foundation for Table 3, that gives qualitative recommendations on when harmonic measurements on IVTs can be performed.

This table was published in the technical brochure 596 by Cigré (2014). The brochure does not recommend using a frequency response curve as a calibration tool for measurements of harmonics above the critical frequency. This is because the error above the critical frequency depends on many factors such as voltage, temperature, and burden, and can therefore vary significantly.

Table 3 - Recommendations on when measurements

of voltage harmonics can be performed on an IVT at different voltage levels with an assumed maximum error of 1%. Source: (Cigré, 2014)

	Voltage level	2^{nd} to 7^{th} Harmonic	8th to 20^{th} Harmonic	21^{st} to 50^{th} Harmonic
MV	10 kV	Yes	Yes	Yes
	20 kV	Yes	Yes	Uncertain
	30 kV	Yes	No	No
HV	60 kV	Yes	Yes	Uncertain
	110 kV	Yes	Uncertain	No
EHV	220 kV	Uncertain	No	No

2.5.1.2 Capacitive voltage transformer

A capacitive voltage transformer (CVT) is generally used on voltage levels higher than 145 kV and consists of two parts, a capacitive voltage divider (CVD) and an electromagnetic unit (ABB, 2015). The CVD gives a lower voltage level according to the rule of voltage division in Equation 18. The electromagnetic unit (EMU) consists of a transformer and a reactor, which are used to compensate for the capacitive phase shift generated in the CVD and further decrease the voltage to safe levels for measurement. The transformer inside the EMU works on the same principles as the IVT described in 2.5.1.1. By tuning the EMU correctly according to Equation 16, the reactive voltage drop will be cancelled leaving only the resistive part.

$$2\pi fL = \frac{1}{2\pi fC} \tag{16}$$

Due to this tuning, the CVT will only give low errors for the fundamental frequency. A change in frequency could generate large errors in both ratio and phase due to resonance between the capacitances and inductances (ABB, 2015). The technical brochure 596 by Cigré (2014) states that CVTs are not suitable for harmonic measurements due to the exact tuning around the fundamental frequency. Standards guarantee a good accuracy for frequencies between 99% to 101% of rated frequency for metering purposes and 96% to 102% for protective purposes (IEC, 2011).

Figure 16 illustrates an example of a frequency response of a 275 kV CVT with three different burdens (Zhao, 2013). Xiao et al. (2004) have compared the measurement of the 13^{th} harmonic on a CVT and a measurement on a capacitive tap, explained later, and the result can be seen in Figure 17.

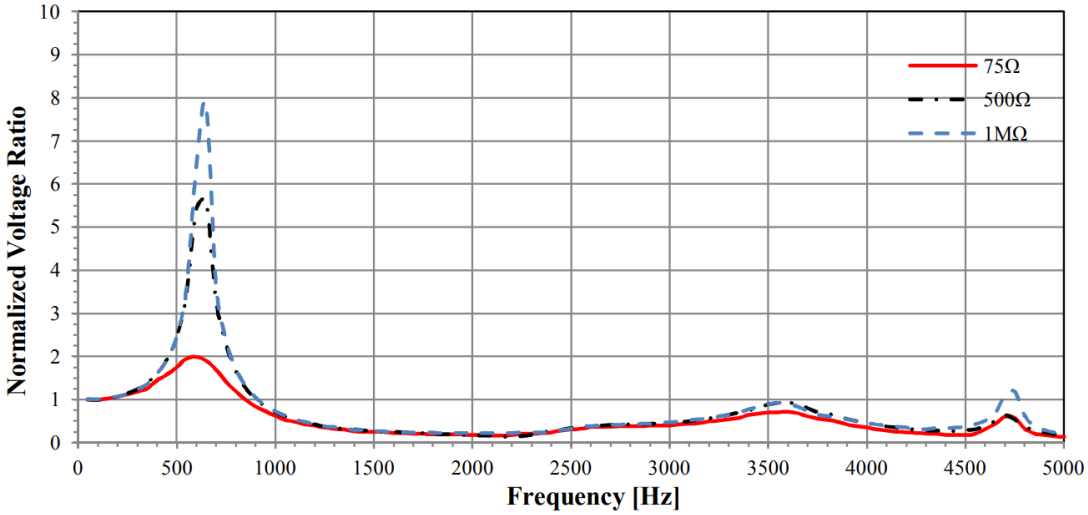

Figure 16 - Example of frequence response of a 275 kV CVT with three different burdens connected to the secondary winding. Source: (Zhao, 2013)

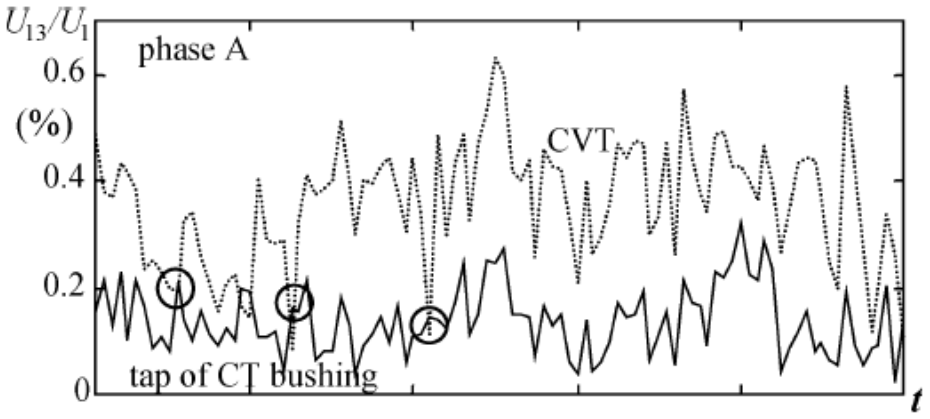

Figure 17 - Comparison of 13th harmonic (650Hz) measured on a CVT and the capacitive tap on a current transformer. Source: (Xiao et al., 2004)

2.5.1.3 Current measurements

Current measurements on high voltages also require some special techniques. However, the main focus in this thesis has been voltage measurements and therefore will not current measurements be described in as much detail as the voltage measurements. An inductive current transformer (CT) works on the same principle as described in 2.2.2 and can be used for current measurements. A high current is transformed to a lower current according to Equation 1, which then can be measured with an appropriate instrument (Wildi, 1991).

2.6 MEASURING VOLTAGE HARMONICS AT HIGH VOLTAGE LEVELS

Due to the poor frequency range of traditional measurement transformers explained in Section 2.5.1, other techniques are necessary to measure harmonics accurately. There are multiple methods for measuring harmonics on high voltages, but this thesis will focus on three methods.

2.6.1 Resistive-capacitive voltage divider

For the most accurate voltage harmonic measurements, a resistive-capacitive voltage divider (RCVD) is recommended (Dewayalage, 2025). A RCVD consists of a capacitance in parallel with a resistance, connected in series to a second group of resistance and capacitance, illustrated in Figure 18. To achieve high accuracy across a wide frequency range, well-defined capacitors and resistors with low parasitic inductances are needed. The values of the components need to satisfy Equation 17 in order to get a good accuracy in the whole frequency range (Zong et al., 2010; Sperling and Schegner, 2013). The precise design process combined with the high-quality requirements of the components makes this type of voltage sensor more expensive compared to conventional measurement transformers such as IVTs and CVTs (Dewayalage, 2025).

There is also a possibility to omit the resistors in a RCVD and only use the capacitors, resulting in a capacitive voltage divider (CVD). A CVD has similar high-frequency characteristics to a RCVD but loses accuracy as the frequency approaches zero hertz (Sperling and Schegner, 2013).

$$R_1 C_1 = R_2 C_2 \tag{17}$$

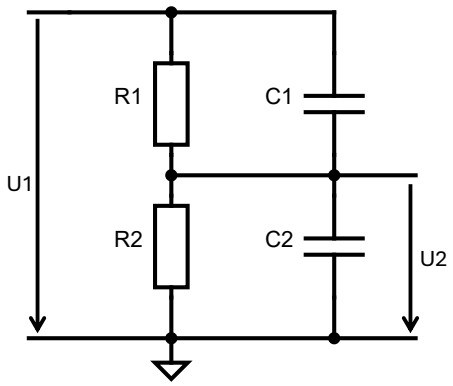

Figure 18 - Circuit of a RCVD. The power system voltage is denoted as U1, and measurements are taken across U2.

2.6.2 Measurement using a capacitive tap

High-frequency voltage harmonics can be measured using the capacitive tap on a current transformer or the bushings on power transformers (Xiao et al., 2004; Tenbohlen et al., 2018; Carlsson, Holmberg and Östlund, n.d.). A capacitive tap is a connection point used for measuring the dissipation factor, described in Section 2.4.3.3, on high voltage equipment with a condenser core as insulation. A condenser core is designed to control the internal electric field by placing layers of thin conductive foil between the oil or resin impregnated paper (Murty, 2017). These foils form a high voltage capacitor between the conductor and ground potential. An explanation of this measurement method utilized on a current transformer is described by Xiao et al. (2004). The principle of the method is to connect a capacitor in series with the outer foil layer of the condenser core and ground, forming a capacitive voltage divider suitable for harmonic measurements. For this method to function properly, the capacitance between the inner and outer foil of the current transformer needs to be known. According to Xiao et al. (2004), this value is about 650 pF for a 500 kV current transformer. The capacitor placed in series with the foils should have a capacitance such that the voltage over it is around

50 to 100 V. This value can be calculated with Equation 18, where C_1 is the capacitance between the inner and outer foil, C_2 is the capacitance of the series connected capacitor and U_1 is the system voltage. To protect the secondary capacitor from transient overvoltage, its voltage rating should be at least four times larger than the calculated measurement voltage. Measurements can then be performed over the capacitor connected in series, with a suitable instrument. The same principle can be applied to a transformer bushing. This method could in theory give accurate measurement of voltage harmonics in the supraharmonic frequency range (Tenbohlen et al., 2018).

$$U_2 = U_1 \frac{C_1}{C_1 + C_2} \tag{18}$$

There are, however, some problems when utilizing this method. Firstly, to safely connect the measurement capacitor, de-energization is necessary, which must be planned in advance. To address this issue, Xiao et al. (2004) suggests that manufacturers implement a built-in capacitor that could be used for harmonic measurements. Another significant drawback is that the voltage signal obtained from the capacitive tap does not have a well-defined reference. This will result in a measurement that will fluctuate over time and can therefore only measure harmonic amplitudes relative to each other. For example, it can indicate that the amplitude of one harmonic is twice that of another, but it cannot be used to determine the actual voltage of a specific harmonic. This issue can be mitigated by combining the measured signal from the capacitive tap with a traditional voltage transformer. According to Carlsson, Holmberg and Östlund (n.d.) can a measurement system be designed where the signal from the capacitive tap automatically calibrates itself from the measurements from a regular voltage transformer. In their system, an IVT was used as a reference signal to calibrate the measurement from the capacitive tap. The regular voltage transformer has a well-defined accuracy around the fundamental frequency. The known amplitude of the fundamental frequency is therefore used to calibrate the relative harmonic amplitudes measured on the capacitive tap.

Some factors that might affect the results are temperature variations and aging of the insulation material. These factors have been investigated by Tenbohlen et al. (2018), and the results indicate that the maximum error should still remain below the 5% limit stated in IEC 61000-4-7.

2.6.3 Power quality sensors for CVTs

As described in Section 2.5.1.2, CVTs cannot be used for harmonic measurements due to their tuned frequency calibration. It is possible to install an additional measurement circuit to the CVT, and harmonic measurements with acceptable accuracy up to at least 5 kHz can be performed. PQSensor™ is an example of a patented module that could be fitted onto existing CVTs (BVM Systems Limited, n.d.). This is utilized by connecting two current sensors on the grounded conductor as illustrated in Figure 19. The benefit of installing the current sensors at these locations is that no specific insulation is needed since both of the current sensors are installed at ground potential.

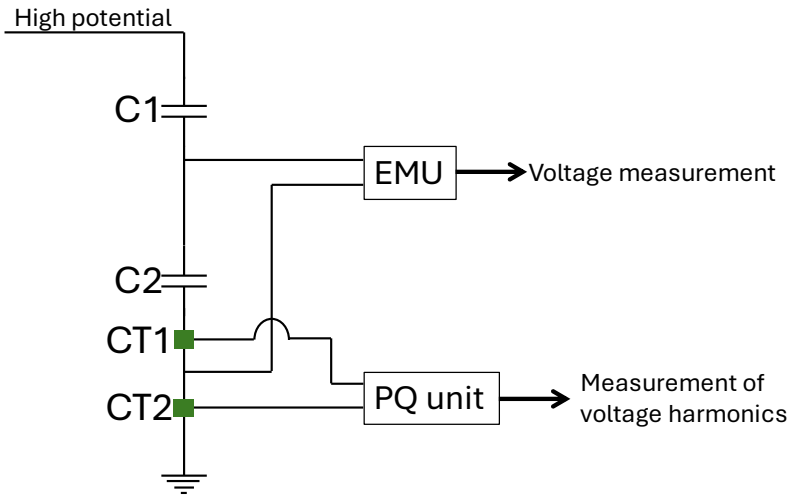

Figure 19 - Principal schematic of the PQSensor™ module. C1 and C2 represent the capacitances in the CVT, while CT1 and CT2 are current transformers. Figure inspired by (Zhao et al., 2010).

Since the two capacitances in the CVT are known, the voltage drop of each capacitor can be calculated if the current flowing through them is known. The first CT, CT1, measures the current in C_2 and the second CT, CT2, measures the sum of the current from C_2 and the EMU hence the total current flowing thru C_1. When the two currents are known, the voltage drops over C_1 and C_2 can be calculated according to Equation 19. U_f is the voltage amplitude with frequency f, $C1$ and C_2 are the capacitance of the two capacitors and $I_{MCT1}(f)$ and $I_{MCT2}(f)$ are the current with frequency f measured at the two current sensors (Dewayalage et al., 2024).

$$U_f(f) = \frac{1}{2\pi f C_1}\left(I_{CT1}(f) + I_{CT2}(f)\right) + \frac{1}{2\pi f C_2} I_{CT1}(f) \tag{19}$$

2.7 HARMONICS' EFFECTS ON ELECTRICAL EQUIPMENT

The effects of harmonics in the power system are mainly increased losses, which lead to elevated operating temperature. These losses are well documented in the literature and will therefore only be briefly summarized here. When the harmonic frequencies increase, some effects can be more severe, which will be explained in more detail.

2.7.1 Generators

The primary issue associated with harmonics in generators is the additional heat generated by current harmonics. This heat is mainly generated within the windings and iron cores in the form of increased copper losses and eddy current losses, as described in Section 2.4.3. Other typical symptoms include torque pulsations caused by current harmonics, as well as increased vibration and noise (Thunberg, 2001).

2.7.2 Power transformers

As for the rotating machines, the primary concern related to harmonics in power transformers is the generation of excess heat. These losses are mainly copper losses and eddy current losses. Voltage harmonics also increase the stress on insulation material in the transformer due to dielectric losses explained in Section 2.4.3.3 (Thunberg, 2001).

2.7.3 Relay protection

High levels of harmonic distortion can affect relay protections in negative ways. One example is the zero-crossing detection used by digital relays, which may lead to incorrect timing or misinterpretation of system conditions. This can result in unintended tripping of a relay when no actual fault is present or in the worst case, failure to trip during a genuine fault condition. However, the required harmonic levels for these faults to occur are normally much higher than the harmonic levels that normally are found at HPPs (Thunberg, 2001; Benjamin and Jain, 2018).

2.7.4 Measurement transformers

The effects of harmonics on voltage measurement transformers were discussed in Section 2.5.1. Therefore, this section will instead focus on CTs.

Distorted current on the primary side of a CT can saturate the iron and therefore produce a distorted current on the secondary side. When the THD of the primary side increases, the RMS current increases according to Equation 5. Anuar et al. (2012) tested a CT with a 7.5/1 A ratio, both in laboratory and in simulations. Their findings show that the error between both sides is relatively small until the iron core got saturated at the knee point from which the error increased drastically. Nisja (2018) conducted a similar test with comparable results. Nisja (2018) also exemplified how core saturation in CTs can cause differential protection of a transformer to trip even if no fault occurred. Differential protection relies on comparing the current on the primary and secondary side of a transformer. If an unusual difference is detected, the relay assumes a fault and disconnects the transformer. In their example, an unusual difference was observed when the THD on the secondary side increased, causing the differential relay to trip even though no actual fault was present. This occurred since the THD of the secondary side of the transformer is higher than on the primary side due to the damping of harmonics in the power transformer.

3 SUPRAHARMONICS

As more frequency converters are integrated into the power system, supraharmonic emissions are becoming increasingly common. Supraharmonics refers to harmonic frequencies in the range from 2 kHz to 150 kHz (Rajkumar, Balasubramanian and Kathirvelu, 2024). These frequencies are often aligned with the switching frequencies of frequency converters (Paulsson et al., 2003). While the amplitudes of these harmonic emissions are typically not directly harmful, resonances within the system can amplify them, resulting in significant voltage and current harmonic amplitudes that may lead to potential problems. In some cases, MV cable terminations have failed within hours due to supraharmonic voltages (Paulsson et al., 2003). Additionally, high-frequency harmonics have been found to significantly accelerate aging processes in equipment due to increased losses, such as insulation in distribution transformers (Yaghoobi et al., 2020).

3.1 SOURCES OF SUPRAHARMONICS

Supraharmonics can be generated by many sources, where the majority can be found in the LV grids. These sources can be generalized as power electronics that use high frequency switching to generate a specific waveform. As described in Section 2.3.2.1, PWM switching can generate harmonics around the switching frequency and its multiples. Some sources of supraharmonics are wind- and solar power, electric vehicle charges, and lightning systems (Rajkumar, Balasubramanian and Kathirvelu, 2024). Supraharmonics are often contained within LV grids but can be transferred to MV grids under certain conditions. This thesis will focus on the type of sources that are most likely to cause problems in MV and HV grids where a large portion of HPPs is connected.

Wind power plants are one significant source of supraharmonics in the MV grids due to their high power output. The transformers combined with filters filter out a large part of the supraharmonic components, but some are still transferred into the MV grid. Behkesh Noshahr, (2016) studied supraharmonic emissions from a PMSG wind turbine with a frequency converter and showed that supraharmonic components in the range between 2 kHz and 30 kHz could be detected in a 20 kV distribution line over a distance of 28 km. The study by Behkesh Noshahr, (2016) builds on a simulation in MATLAB with a switching frequency of 3.3 kHz and a total power of 1.5 MW. Alizade and Noshahr, (2017) showed in another paper that DFIG wind turbines also produce supraharmonics and significant levels of electrical background noise that cannot be overlooked.

3.2 PROPAGATION OF SUPRAHARMONICS

Supraharmonics can propagate in MV grids, Novitskiy, Schlegel and Westermann, (2018) measured supraharmonic voltages in a 20 kV distribution grid and showed that supraharmonic voltages propagated 16 km in the grid. How well a supraharmonic component of a specific frequency can propagate in the grid depends on the grid's impedance that could vary significantly. If the impedance aligns with a resonance frequency, even a minor current can result in a considerable voltage level according to Equation 3. The size of the grid has an impact on the resonance frequency as well. Larger grids have more resonance frequencies but with a lower amplitude compared with smaller grids, that have fewer but larger resonance frequencies

(Letha et al., 2021). Supraharmonics can also propagate some distances in EHV grids. Zolett and Leborgne (2020) investigated how supraharmonics propagate in a 230 kV transmission grid in Brazil. The results show that supraharmonics can propagate in transmission grids, but the levels are decreasing with distance. The design of the grid, including substations, load characteristics, capacitor banks, and short circuit capacity, contributed to reducing the supraharmonics levels.

How well supraharmonics can transfer between voltage levels partly depends on the transformer connecting them, in combination with other factors such as grid impedances. Duan et al. (2021) have investigated how well different supraharmonics are propagating through a distribution transformer. This was performed by a simulation with a frequency dependent transformer model with a ratio of 10/0.4 kV that was operating in different conditions with supraharmonics frequencies up to 50 kHz. A frequency dependent transformer model includes parameters such as stray capacitances between windings. The conclusions are that propagation is frequency dependent due to the stray capacitances within the transformer. A maximum gain is reached when a parallel resonance occurs, and a minimal gain occurs at series resonance. Slangen et al. (2023) reached similar conclusions in a laboratory setup, measuring frequencies up to 10 kHz. Their findings indicate that the transfer ratio of supraharmonic voltages from the LV side to the MV side of a distribution transformer can range from 0.01 to 1, depending on the frequency. Transfer ratio is how much the amplitude changes with respect to the winding factor. The ratio from MV to LV was 1 to 3, meaning that some frequencies could be amplified three times after the transfer. The conclusion is that most supraharmonic components are damped when propagating from LV to MV, while more components could be transferred from the MV side to the LV side.

3.3 EFFECTS OF SUPRAHARMONICS

Supraharmonics can affect power systems in several ways. This section will focus on how a HPP could be affected. Many of the issues are similar to those caused by lower frequency harmonics described in Section 2.7. However, MV cable termination is an exception, as it can be particularly sensitive to supraharmonic voltages.

3.3.1 Increased losses

A common issue of supraharmonics is the increased losses due to the higher frequencies. Many types of losses in the power system, some of which are described in Section 2.4.3, are frequency dependent. This implies that a supraharmonic component, even with a low amplitude, can cause significant losses if its frequency is high. For instance, eddy current losses increase proportionally to the square of the frequency, as shown in Equation 13. Some examples from different studies are presented below.

Conductors in cables and windings in transformers and generators will suffer the same type of losses from supraharmonics as it does from traditional harmonics. Novitskiy, Schlegel and Westermann (2020) estimated the power losses caused by supraharmonics in a MV cable. This was done by measuring the supraharmonic currents and voltages up to a frequency of 9 kHz, and then calculating the losses using Equations 7 and 12 as a foundation. These measurement results were then verified with computer simulations. The results show that the losses caused by supraharmonic currents can reach several percent of the losses caused by the fundamental

frequency and exceed 10% of the losses caused by conventional low-frequency harmonics. The authors therefore recommend considering supraharmonics for a precise estimation for power losses were switching power electronics, such as frequency converters, are present in the grid.

Yaghoobi et al. (2020) have investigated how supraharmonic currents up to 9 kHz can increase losses in distribution transformers. A few locations were investigated, one of which was a 1400 kVA distribution transformer with a voltage ratio of 11/0.4 kV with two secondary windings. A solar power system with a maximum apparent power of 720 kVA is connected to each of the secondary windings. For the described system, supraharmonic currents up to 9 kHz caused an accelerated aging of 22% on the insulating material in the transformer. Two peaks of current harmonics around the switching frequency of 3 kHz are also present. These peaks generated eddy current losses amounting to 33% of the eddy current losses generated by the fundamental frequency current, and would not be noticed if the supraharmonic frequencies were not measured. This percentage factor was calculated with Equation 20, were I_h and I_1 represent the current of the harmonic component and the fundamental current in amperes, respectively, and h is the harmonic order.

$$k_{loss} = \left(\frac{I_h}{I_1}\right)^2 \cdot h^2 \tag{20}$$

3.3.2 Failure of MV cable termination

MV cable terminations can be sensitive to supraharmonic voltages because they are required to withstand higher voltages and electric field stresses compared to LV systems. Additionally, a simpler field control system is often used compared to HV and EHV terminations. Supraharmonic voltages could cause losses in the terminations that could lead to accelerated aging and failures. This is the case for the non-geometric type of cable termination, while the geometric type does not have the same problem due to a different field control system (Paulsson et al., 2003; Banerjee, 2008). The heating is generated by dielectric losses from supraharmonic voltages. An example of this occurred at the Eagle Pass converter station, a back-to-back frequency converter that connects two AC grids at the border between the USA and Mexico. A failure related to supraharmonic voltages was observed at the station and was later recreated in a laboratory to understand the scenario that occurred. A paper with the findings was then published by Paulsson et al. (2003).

When the cable termination was exposed to supraharmonic voltages, dielectric losses in the insulation and resistive losses in the stress grading material led to localized heating around the point of contact between the insulation, semi-conducing layer and the stress grading layer visible in Figure 4. As the temperature increased, silicon grease at the interface between the insulation and stress grading layer began to dry out and migrate through the stress grading layer, leaving a cavity at the interface. This cavity combined with the high electric field initiated partial discharges, further increasing the heating and deterioration of the material, ultimately leading to a complete breakdown of the termination. Measurements indicated that the most severe supraharmonic frequency was at 12.4 kHz, ten times the switching frequency of the frequency converter. At this frequency, the supraharmonic voltage ranged from 13% to 40% of the 17.9 kV fundamental voltage, depending on how the switching was conducted. These very high voltages were possible due to local resonance that was excited by the switching frequency of the frequency converter. To solve this problem, all cable terminations at the site

were replaced by a geometric type that can handle the electric fields better than the non-geometric type. A resistor-capacitor (RC) filter designed to damp frequencies at 12.4 kHz was also installed on site.

A method for evaluating the risk of failure due to supraharmonic voltage was presented by Espín-Delgado et al. (2020). This method relies on measurements of supraharmonic voltages, which require special equipment as described in Section 2.5 and 2.6. However, alternative methods can provide an indication of potential failures. Thermal imaging is a method for detecting abnormal heat spots on cable terminations. If a hotspot is observed at the point where the insulation, semiconductive layer, and the stress grading layer meet, it may indicate the presence of supraharmonic voltages. An example of how a cable termination affected by supraharmonic voltages appears in a thermal image is shown in Figure 20 (Banerjee, 2008). Another useful tool for identifying damaged cable terminations is an acoustic camera (FlirSystems, 2021). Sound generated by the energy released during a partial discharge can be detected and visualized using an acoustic camera. An example of this can be seen in Figure 21. None of these two methods can guarantee that supraharmonic voltages are the cause of the observed heat and sound emissions. Similar observations might as well be a result of something else. For example, poor workmanship during installation accounts for 66% of all failures on MV cable terminations and could show the same symptoms as supraharmonics (Higinbotham, 2019).

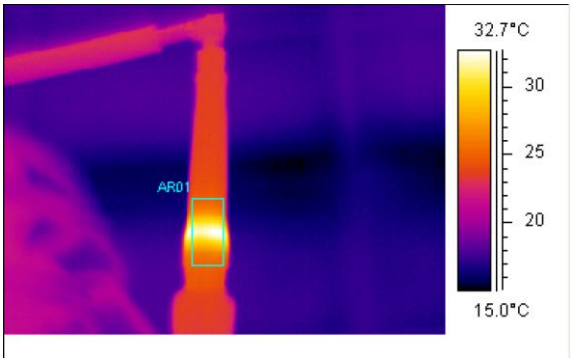

Figure 20 - Heating of a cable termination exposed to supraharmonic voltage.
Source: (Banerjee, 2008)

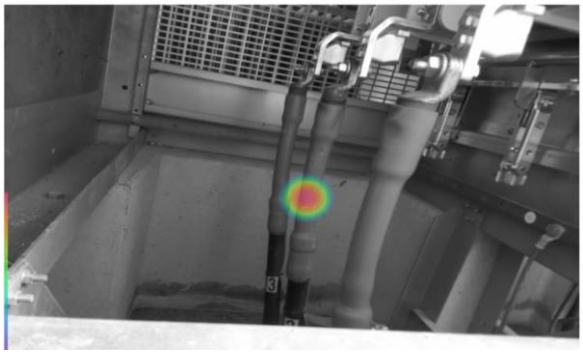

Figure 21 - Acoustic sounds created by PD activity in cable termination.
Source: (TEquipment, 2025)

4 METHODOLOGY

Measurement of harmonics has been carried out at three different HPPs and data from one HPP has been provided from another source. This data has then been analyzed to answer the research questions. Each HPP has been assigned a number from one to four for anonymization purposes. HPP 1 to 3 were used for weeklong voltage measurements, while the fourth HPP was designated for current measurements at a battery system.

4.1 EQUIPMENT AND SOFTWARE

Suitable equipment is necessary to perform harmonic measurements. This section outlines the equipment used for these measurements.

4.1.1 Measurement equipment

Two different measurement equipment was used for the measurements, the Dranetz PX5 which has been used for the voltage measurements and the Dranetz HDPQ Plus which has been used for the designated current measurement. Apart from these instruments, some other instruments have been used to measure the data which was provided. All of these instruments meet the IEC 61000-4-30 class A standard.

4.1.2 Software

Several software programs have been used, with the most important being DranView. DranView is a data analysis software used with equipment made by Dranetz. It is used to visualize results, generate reports, and export data from measurements performed with Dranetz equipment. In this thesis, it has mainly been used as a tool to export data for use with MATLAB.

4.2 MEASUREMENT PROCEDURES

There are some variations in the measurement procedures at each HPP due to limitations in what could be measured at each location. The preferred method at each HPP is presented in this section. A brief explanation of some relevant standards will also be presented.

4.2.1 Standards

Two standards are particularly relevant for the harmonic measurements conducted in this thesis. IEC 61000-4-30 is a standard defining methods for power quality measurements in AC grids with a frequency of 50 Hz or 60 Hz. This standard specifies, among other things, the requirements for measurement equipment and how data should be recorded. All measurements in this thesis were performed with class A instruments.

IEC 61000-4-7 is an international standard that defines measurement techniques for harmonics and interharmonics up to a frequency of 9 kHz in power supply systems. It also defines accuracy requirements for measurement equipment for different classes of accuracy. According to this standard, the maximum allowed measurement error for a class A instrument is 5%.

4.2.2 Voltage measurement

Since the measurements in this thesis have been performed on the MV level or higher, measurement transformers have been used. The general approach for the voltage measurement is to measure the phase to neutral voltages as shown in Figure 22 where M represents the voltage measurement points followed by the letters A, B and C which represent each phase. Measurements were performed on the metering circuit for the best accuracy. Scaling values in the instrument were chosen according to the winding factor at each location. The measurements are based on ten-cycle windows according to IEC 61000-4-30. Every ten-minutes, the average, highest, and lowest RMS values for each harmonic up to the 49th harmonic are recorded. Measurements for IEC 50160 compliance were conducted for one week at each location.

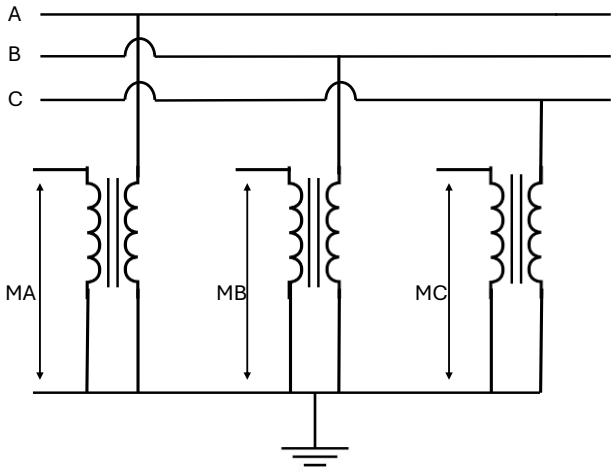

Figure 22 - Measurement setup for measurement transformers. A, B and C represent each phase on the primary side, and MA, MB and MB represent the measurement points.

4.2.3 Current measurement

Current measurements have been performed either directly on the power cable or on the secondary of a current transformer. The current probes are of a clamp-on type, meaning that those can be connected without a disconnection of the measurement circuit. Each current measurement will be described separately.

4.2.4 Production data

Production data for the HPPs were collected internally from Fortum. Daily production data from three wind turbines in a wind farm near a HPP were collected from a public source. The combined average output of these three turbines was then multiplied by the total number of turbines in the park to estimate the overall daily production of the park.

4.3 DATA ANALYSIS

Data from the measurements performed with Dranetz instruments are extracted from DranView. Relevant data is then exported into an excel file. The received data for one of the HPPs was in excel format as well. The excel files are then loaded into MATLAB where they are used to produce the figures.

An assumption has been made that all phases have the same harmonic levels, as a balanced three-phase system is assumed. Therefore, only phase A is presented in figures, except for those showing the THD of the voltage, to enhance readability. The figures presenting the THD will show all three phases. Additionally, average values from each ten-minute period are presented unless stated otherwise for the respective figure. All voltage harmonics are presented as a percentage of the fundamental voltage.

4.4 POWER PLANT DESCRIPTION

In this section, the HPPs used in this study will be described. HPP 1 to 3 were used for the weeklong measurement of voltage harmonics in accordance with IEC 50160, and HPP 4 was used for the measurement of current supraharmonics from a battery system.

4.4.1.1 HPP 1

HPP 1 is a small HPP with a rated power of 3.2 MVA, located in a village outside a larger town. The HPP is connected to the local grid at a voltage level of 10 kV.

Measurement at HPP 1

Dranetz PX5 is used at HPP 1 together with the TR2550A current sensor to measure voltage and current on the grid side of the power transformer, illustrated in Figure 23. The voltage measurement has been performed as described in Section 4.2.2, with the winding factor equal to 100. The type of IVT has not been found, so an assumption based on Table 3 has been made that the measurements can be performed up to the 50th harmonic with acceptable accuracy. Currents were measured on the secondary circuit of the CT with a winding factor of 40. It was not possible to find the type of current transformer either.

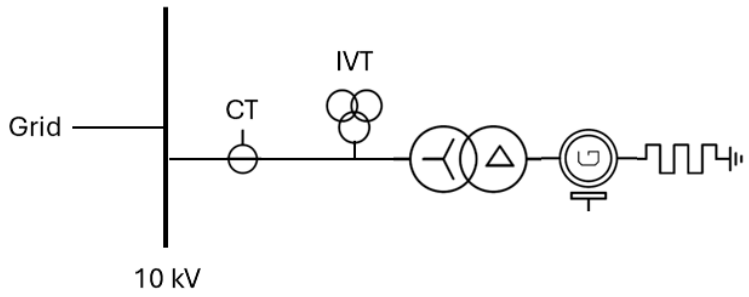

Figure 23 - Simplified schematic of HPP 1. Voltage measurements were performed on the IVT and current measurements on the secondary side of the CT.

4.4.1.2 HPP 2

HPP 2 is a small HPP with a rated power of 3.6 MVA, located in a small village. It is connected to a 50 kV bus, which also connects to four overhead lines. Two of these lines are connected to some diverse loads before it connects to the 130 kV grid approximately 35 km away. One of the remaining lines radially connects two other HPPs located about 50 km away, while the fourth line connects to a wind farm approximately 13 km away. The wind farm has a rated power of 30 MW and consists of 15 DFIG turbines with a rated power of 2 MW each.

Measurement at HPP 2

The Dranetz PX5 was used to measure voltage on the 50 kV bus, using the method described in Section 4.2.2, with a winding factor of 500. A simplified schematic of the site is illustrated in Figure 24. However, it was not possible to measure the current at this location since the IVT and CT owned by Fortum are located in separate buildings.

The IVT used for this measurement is an EMFC 72, manufactured in 1991. This type of IVT is assumed to have a critical frequency of 1.9 kHz with a maximum error of 5%, and a critical frequency of 2.35 kHz with a maximum error of 10%. At the first resonance frequency, the amplitude dips, meaning the actual voltage will be higher than the measured voltage. These assumptions are based on measurements of a similar IVT in the PhD thesis by Dewayalage (2025). However, there are differences between the IVT at HPP 2 and the IVT tested by Dewayalage (2025). The most noticeable difference is the primary voltage rating. The IVT at HPP 2 is rated at $55/\sqrt{3}\ kV$ compared to $65/\sqrt{3}\ kV$. It is important to note that these are only assumptions, and the actual errors are unknown. According to Table 3, the critical frequency for the 1% error is at the 20th harmonic, or 1 kHz.

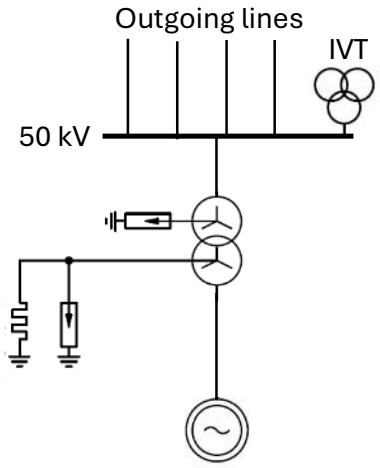

Figure 24 - Simplified overview of HPP 2. Voltage measurements were performed on the IVT.

4.4.1.3 HPP 3

HPP 3 is a large HPP with a rated power of 168 MVA, located in a rural area. It is connected to a switchyard with two voltage levels, 45 kV and 220 kV. The critical frequency for the IVT on the 45 kV bus is unknown. According to Table 3, can measurements up to the 20th harmonic give acceptable results. All measurements from the CVT on the 220 kV bus are assumed to give poor accuracy, according to discussion in Section 2.5.1.2. All measurement data from HPP 3 was obtained from power quality equipment installed on site by the grid operator. The instruments used are class A rated, and the measurements were conducted as described in Section 4.2.2.

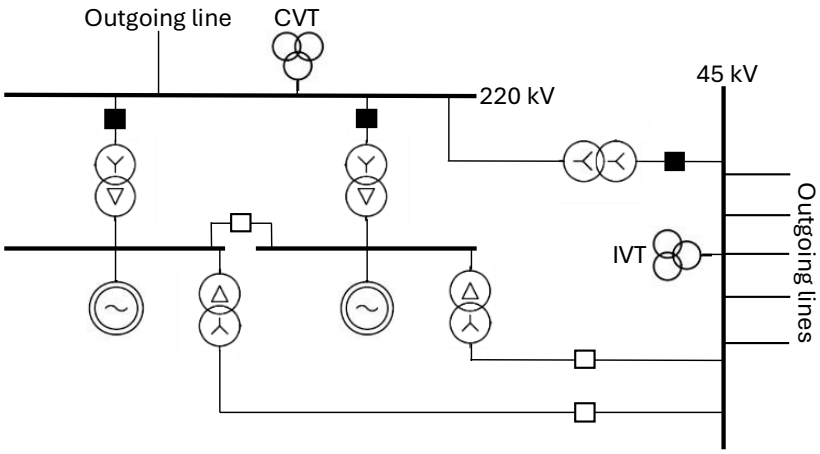

Figure 25 - Simplified overview of HPP 4 during the measurements. Voltage measurements were conducted on both the CVT and IVT. The squares represent switches. Black squares indicate closed switches, while white squares indicate open switches.

4.4.1.4 HPP 4

The goal with this measurement is to investigate whether a battery system generates any significant supraharmonic currents up to 10 kHz. As discussed in Section 3.3.1, supraharmonic currents caused by frequency converters can increase losses in distribution transformers. The battery system at HPP 4 is used for frequency regulation, supplying power to the grid when the frequency is low, and absorbing power when the frequency is high. The system consists of multiple batteries and frequency converters, connected to a 10 kV bus within the HPP, as illustrated in Figure 26.

Measurement at HPP 4

The current from the battery system was measured using the Dranetz HDPQ Xplorer Plus combined with the Dranflex 3000XLB current sensor set to a range of 300A. This setup was selected over a traditional CT to minimize measurement uncertainties. The current was measured on the MV cables marked "*P1*" in Figure 26. The original intention was to measure the current at the location marked "*P2*" in Figure 26. This was not feasible due to practical constraints on the site.

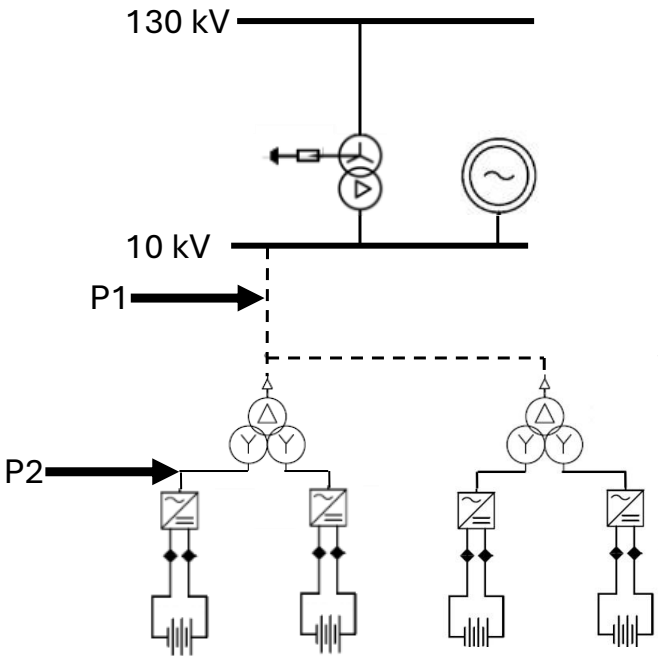

Figure 26 - Schematic of the battery system at HPP 4. Current measurements were performed on the MV cables marked "P1" in the figure. Measuring at "P2" was not possible due to practical constraints on site.

5 RESULTS

In this section, all measurement results will be presented. For HPP 1 to 3, compliance with the IEC 50160 standard will be evaluated as well as any variations of amplitudes of voltage harmonics throughout the week. For HPP 4, supraharmonic currents up to 10 kHz from a battery system will be presented.

5.1 VOLTAGE MEASUREMENTS

In this section, the results from the voltage measurements at HPP 1 to HPP 3 are presented.

5.1.1 HPP 1

At HPP 1, voltage and current harmonics up to the 49th order were measured.

All voltage harmonics are below the allowable limits specified in IEC 50160. The highest 10-minute average for each harmonic is presented in Table 4 below. Additionally, the THD for the voltage remained well below the limit of 8% stated in IEC 50160. The THD fluctuates around 1.5% with an increase during the days from Monday to Friday, illustrated in Figure 27.

Table 4 - Compliance with IEC 50160 regarding individual harmonics at HPP 1. All values are presented as a percentage of the fundamental voltage.

Odd harmonics						**Even harmonics**		
Not multiples of 3			**Multiples of 3**					
Order (h)	Limit (%)	Measured (%)	Order (h)	Limit (%)	Measured (%)	Order (h)	Limit (%)	Measured (%)
5	6,00	1,71	3	5,00	0,18	2	2,00	0,03
7	5,00	1,17	9	1,50	0,07	4	1,00	0,04
11	3,50	0,39	15	0,50	0,04	6 … 24	0,50	0,05
13	3,00	0,33	21	0,50	0,01			
17	2,00	0,13						
19	1,50	0,08						
23	1,50	0,07						
25	1,50	0,06						

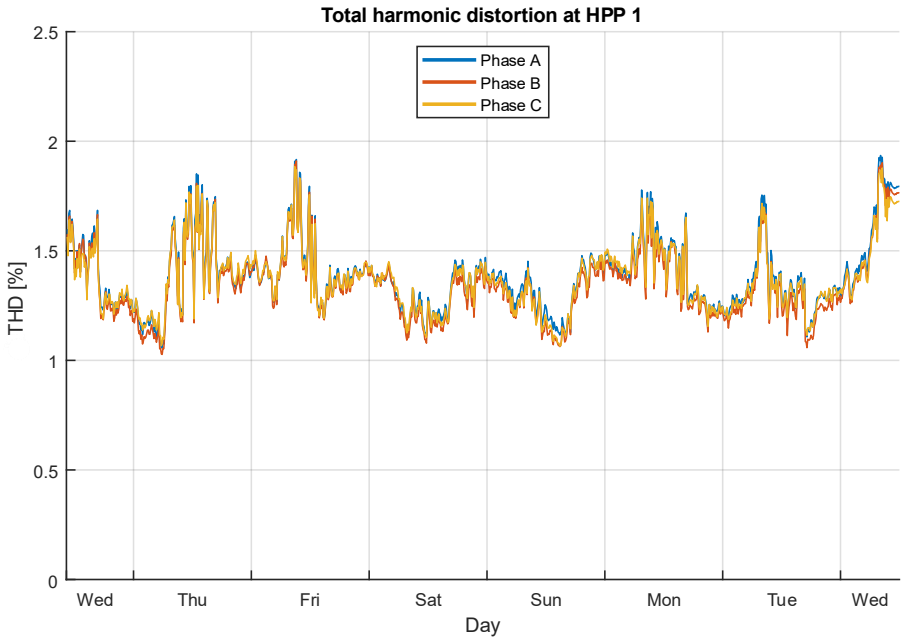

Figure 27 - THD of the voltage at HPP 1 during the week of measurement. The limit, according to IEC 50160, is 8%, indicating a substantial margin before reaching the threshold.

The fifth and seventh harmonics were the largest voltage harmonics observed. The fifth harmonic showed the greatest fluctuation, with peak values occurring during working hours from Monday to Friday, and the lowest levels observed at night. The seventh harmonic was more constant with less fluctuations, its highest values occurred during the nights and the lowest during the days.

Harmonic orders 11, 13, and 17 were the largest after the fifth and seventh, although their magnitudes remained relatively constant and well below the maximum limits specified in the IEC 50160 standard. The five first characteristic harmonics are illustrated in Figure 28 and the corresponding harmonic currents in Appendix A.

All higher-order harmonics can in this case be neglected since these are very small. Figure 29 displays the harmonic spectrum up to the 49^{th} harmonic. The production of both active and reactive power remained almost constant during the week, which can be seen in Appendix A. No voltage interharmonics of interest could be detected, illustrated in Figure 30.

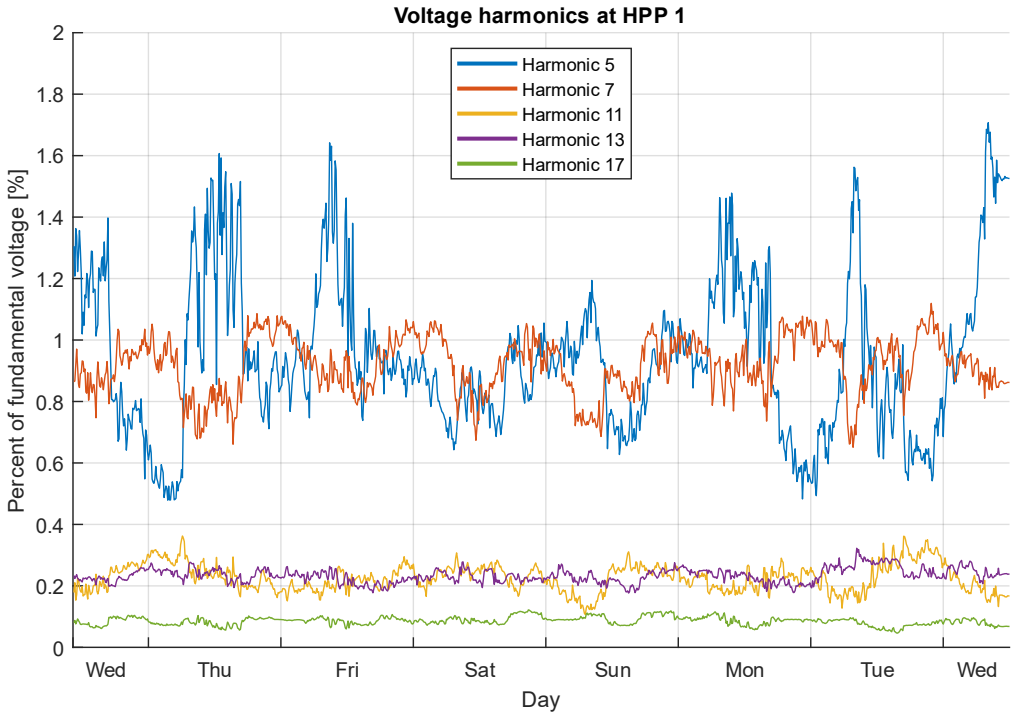

Figure 28 - Amplitude of the five first characteristic voltage harmonics at HPP 1.

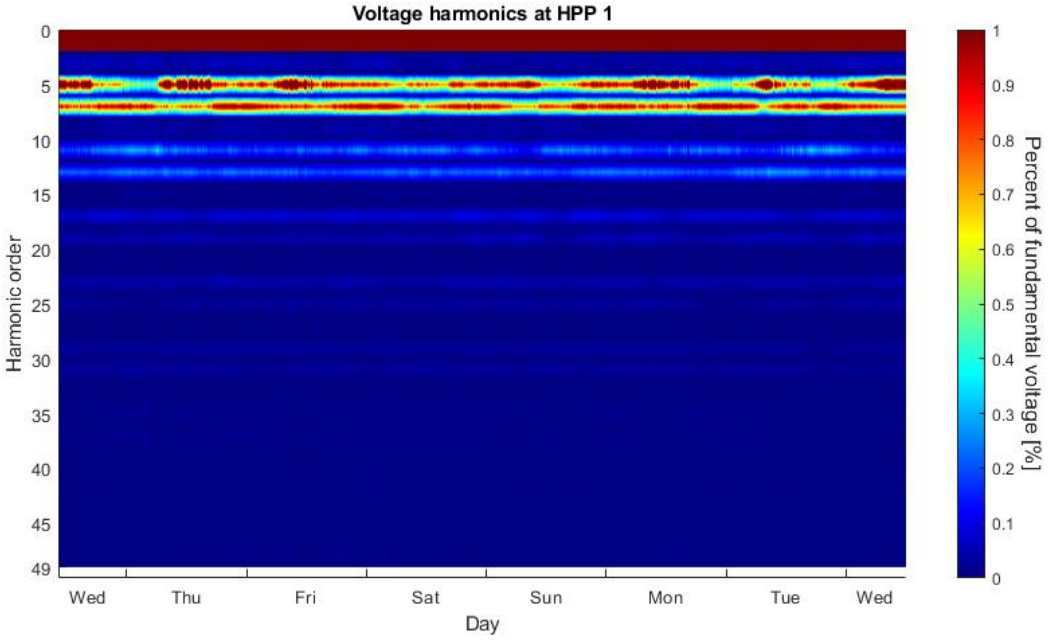

Figure 29 - Harmonic spectrum at HPP 1 where the darkest red symbolizes a harmonic amplitude of 1% of fundamental or higher.

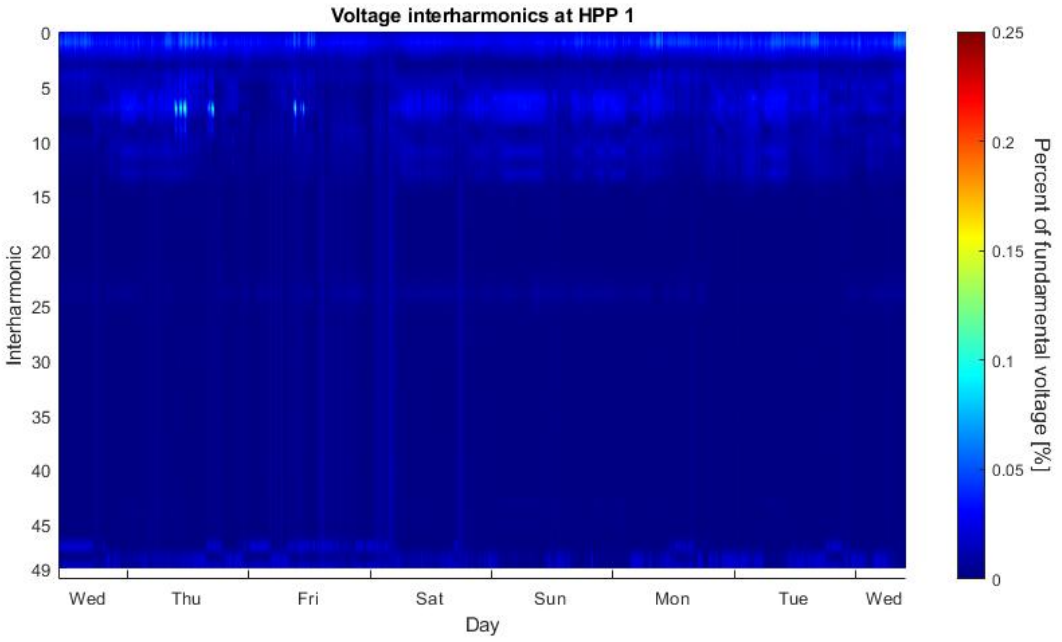

Figure 30 - Voltage interharmonics at HPP 1.

5.1.2 HPP 2

At HPP 2, only voltage was possible to measure due to the layout of the HPP. Voltage harmonics up to the 49th order were measured.

All measured voltage harmonics are below the maximum allowable limits specified in IEC 50160. The maximum 10-minute average for each harmonic is illustrated in Table 5. Although IEC 50160 does not specify limits for harmonics 17, 19, 23, and 25, these were still included in the measurements. No specific limit for the THD has been presented in IEC 50160 since the limit is under consideration. However, the THD limit in IEEE 519 is 5% which is far higher than the maximum THD of around 2% measured at HPP 2. Here the highest THD was reached during the days between Tuesday to Friday. The THD for the whole week is presented in Figure 31.

Table 5 - Compliance with IEC 50160 regarding individual harmonics at HPP 2. All values are presented as a percentage of the fundamental voltage.

Odd harmonics						**Even harmonics**		
Not multiples of 3			**Multiples of 3**					
Order (h)	Limit (%)	Measured (%)	Order (h)	Limit (%)	Measured (%)	Order (h)	Limit (%)	Measured (%)
5	5,00	2,12	3	3,00	0,17	2	1,90	0,07
7	4,00	1,04	9	1,30	0,05	4	1,00	0,07
11	3,00	0,18	15	0,50	0,04	6 … 24	0,50	0,09
13	2,50	0,45	21	0,50	0,04			
17	-	0,10						
19	-	0,13						
23	-	0,16						
25	-	0,31						

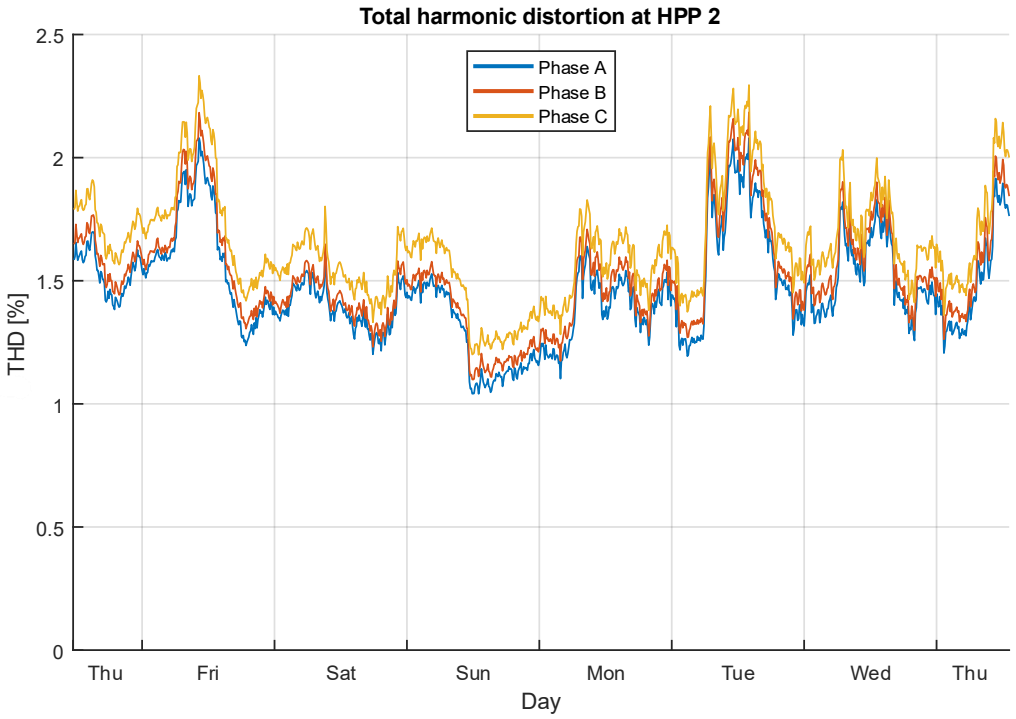

Figure 31 - THD of the voltage at HPP 2.

At HPP 2, the fifth harmonic was the largest, followed by the seventh. The fifth harmonic follows a similar pattern to the THD, with the highest values occurring during weekdays. Harmonics 7, 11, 13, and 17 did not fluctuate as much as the fifth, which can be seen in Figure 32. Higher-order harmonics vary more during the week. Figure 33 shows that there is a distinctive voltage variation for harmonics 25, 29, and 31, where the rest of the harmonics also can be seen. The power production at HPP 2, as well as the nearby HPP and wind farm, can be seen in Figure 34.

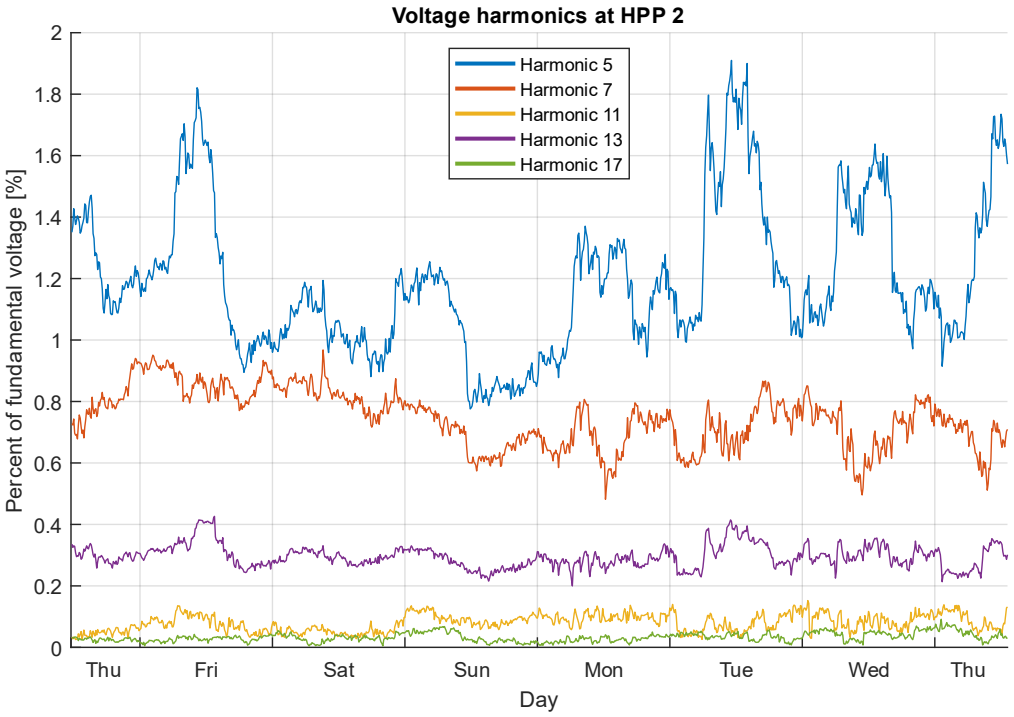

Figure 32 - Amplitude of the five first characteristic voltage harmonics at HPP 2.

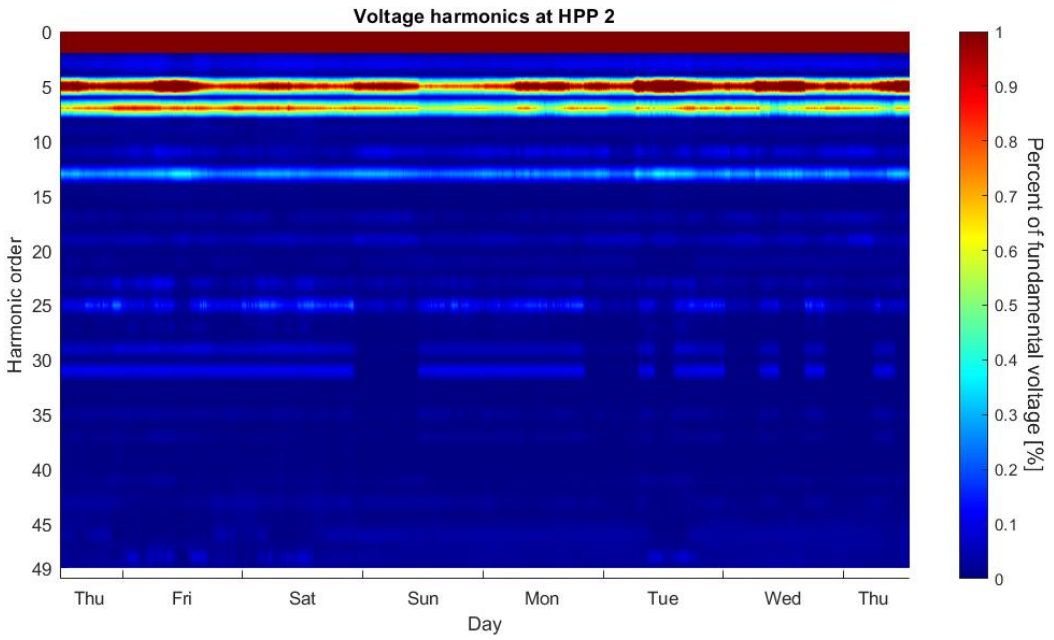

Figure 33 - Harmonic spectrum at HPP 2, where the darkest red symbolizes a harmonic amplitude of 1% of fundamental or higher.

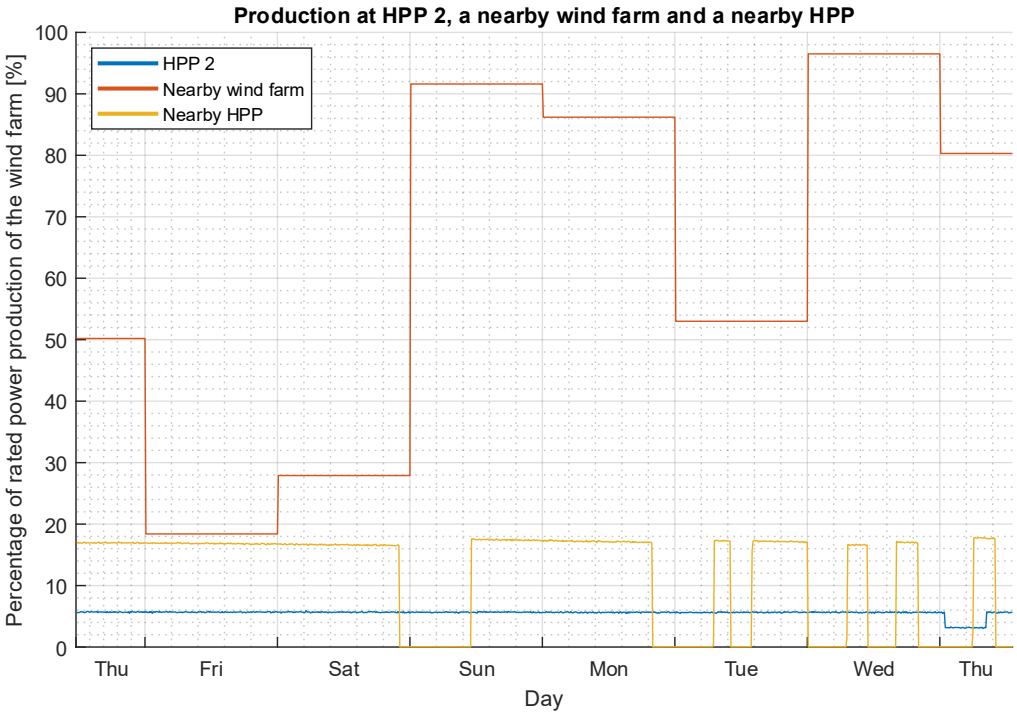

Figure 34 - Production at HPP 2, a nearby HPP, and a nearby wind farm, normalized by the rated power of the nearby wind farm. The wind farm's rated power is significantly higher than the two HPPs.

At HPP 2, several voltage interharmonics of interest were observed. A distinctive wideband of interharmonics appeared between the 45th and 49th orders, along with a noticeable increase in the fifth and seventh interharmonics during periods of higher wind power production, as

shown in Figure 35. The same figure also reveals the presence of interharmonics between the 20th and 25th orders. Figure 36 shows the average voltage interharmonics during the week, voltage interharmonics during high wind production, and voltage interharmonics during low wind production.

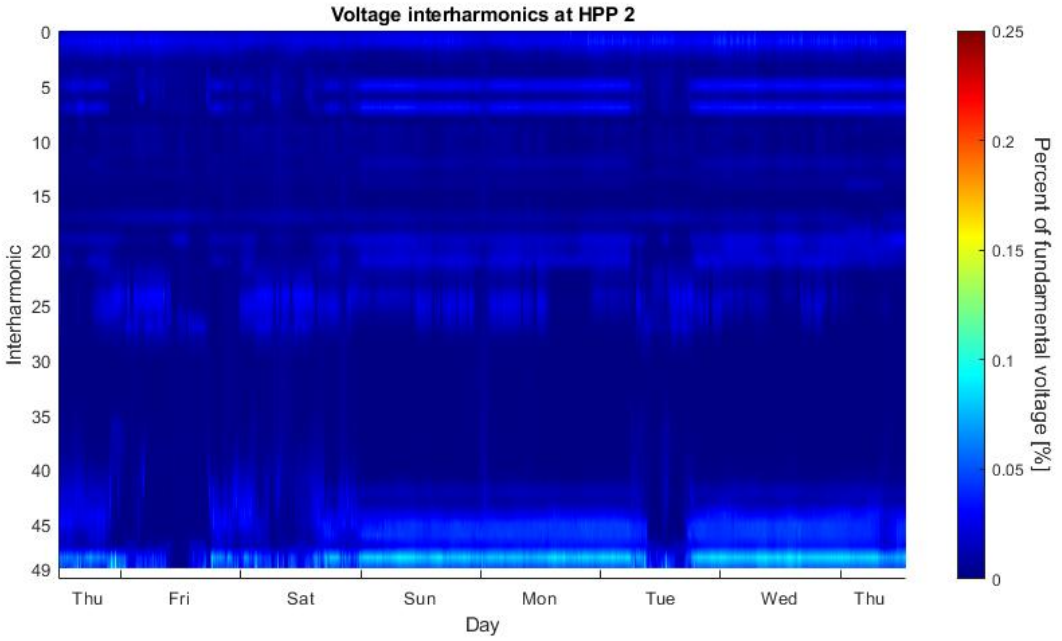

Figure 35 - Voltage interharmonics at HPP 2. All amplitudes are relatively low, but some variations can be observed throughout the week.

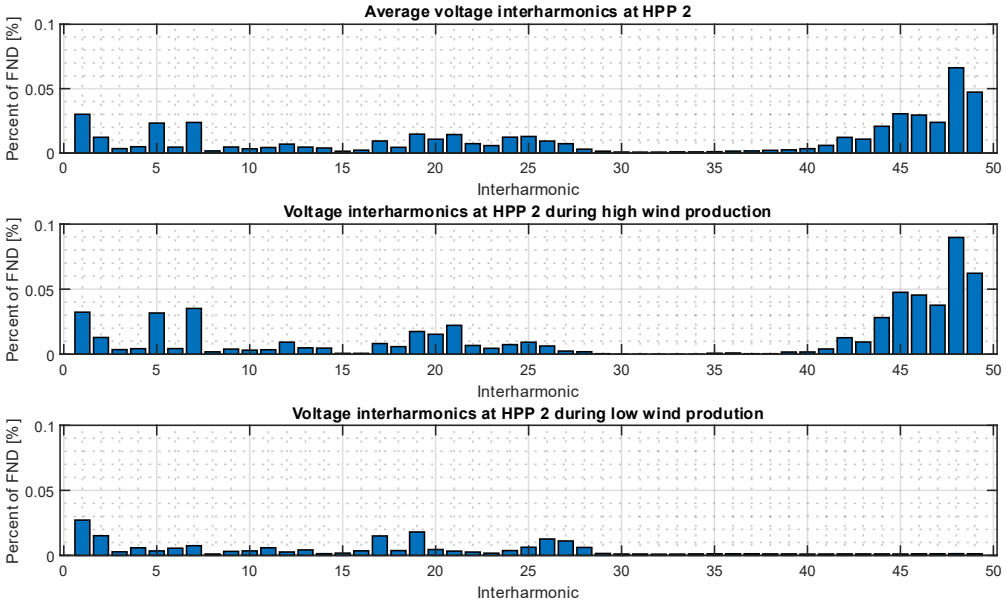

Figure 36 - The top figure shows the average voltage interharmonic levels for the week. The middle one shows the voltage interharmonic levels on Wednesday 08:50 AM during a day when wind production was high. The last shows the voltage interharmonic on Friday 11:00 AM during a day when wind production was low. A clear difference can be seen when the wind production is high respectively low.

5.1.3 HPP 3

Voltage harmonics from the 45 kV bus and 220 kV bus at HPP 3 will be presented here. These measurements were obtained using stationary measurement equipment installed on site. No information regarding the frequency response of the measurement transformers has been found. No interharmonics are evaluated at this HPP since that data was not provided.

5.1.3.1 Measurements on the 45 kV bus

All voltage harmonics are below the maximum allowable limits specified in IEC 50160. Table 6 presents the highest 10-minute average values for each harmonic. Measurements were also conducted for harmonics 17, 19, 23, and 25, despite these not being explicitly limited by IEC 50160. There is however uncertainty of the accuracy of measurements at higher frequencies due to the unknown behavior of the IVT. No specific limit for the THD has been presented in IEC 50160 since the limit is under consideration. But the THD limit in IEEE 519 is 5% which is far higher than the maximum THD of maximum 1% at HPP 3 on the 45 kV bus. THD for the whole week can be seen in Figure 37.

Table 6 - Compliance with IEC 50160 regarding individual harmonics at HPP 3 on the 45 kV bus. All values are presented as a percentage of the fundamental voltage.

Odd harmonics						**Even harmonics**		
Not multiples of 3			**Multiples of 3**					
Order (h)	Limit (%)	Measured (%)	Order (h)	Limit (%)	Measured (%)	Order (h)	Limit (%)	Measured (%)
5	5,00	0,76	3	3,00	0,15	2	1,90	0,02
7	4,00	0,78	9	1,30	0,04	4	1,00	0,07
11	3,00	0,24	15	0,50	0,07	6 … 24	0,50	0,04
13	2,50	0,41	21	0,50	0,02			
17	-	0,23						
19	-	0,13						
23	-	0,11						
25	-	0,09						

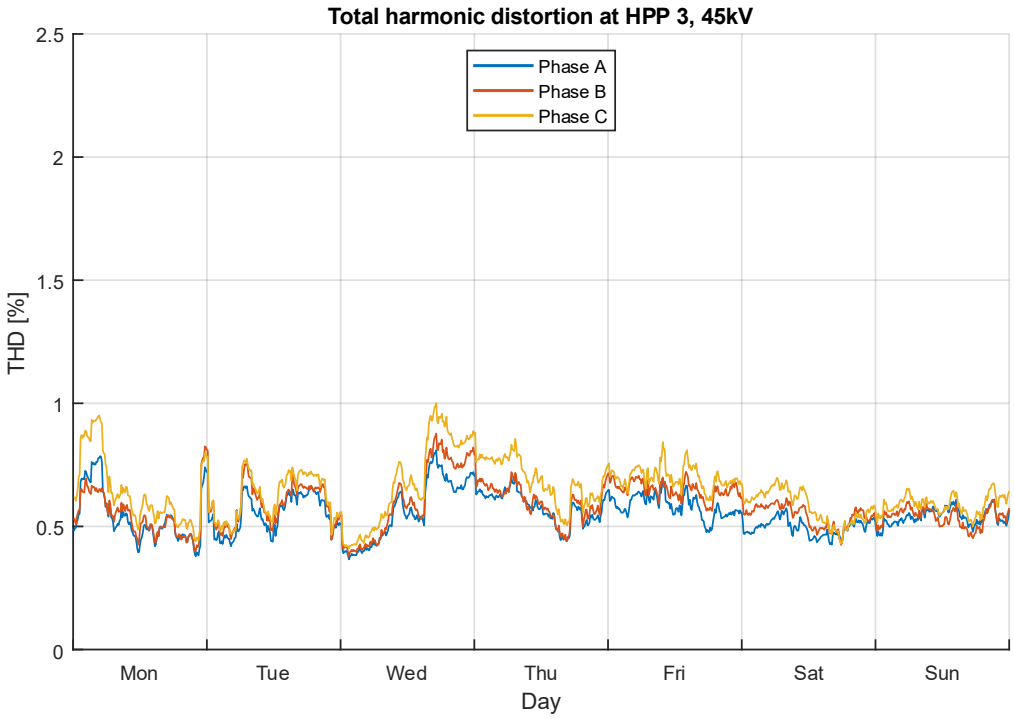

Figure 37 - THD of the voltage at HPP 3 on the 45 kV bus.

The fifth and seventh harmonics were the largest during the week, which can be seen in Figure 38. Higher-order harmonics will be neglected due to their small amplitude and uncertainties of the accuracy of the IVT. All measured harmonics are illustrated in Figure 39. No increase in the THD during weekdays was observed. Production data for HPP 3 is presented in Appendix A.

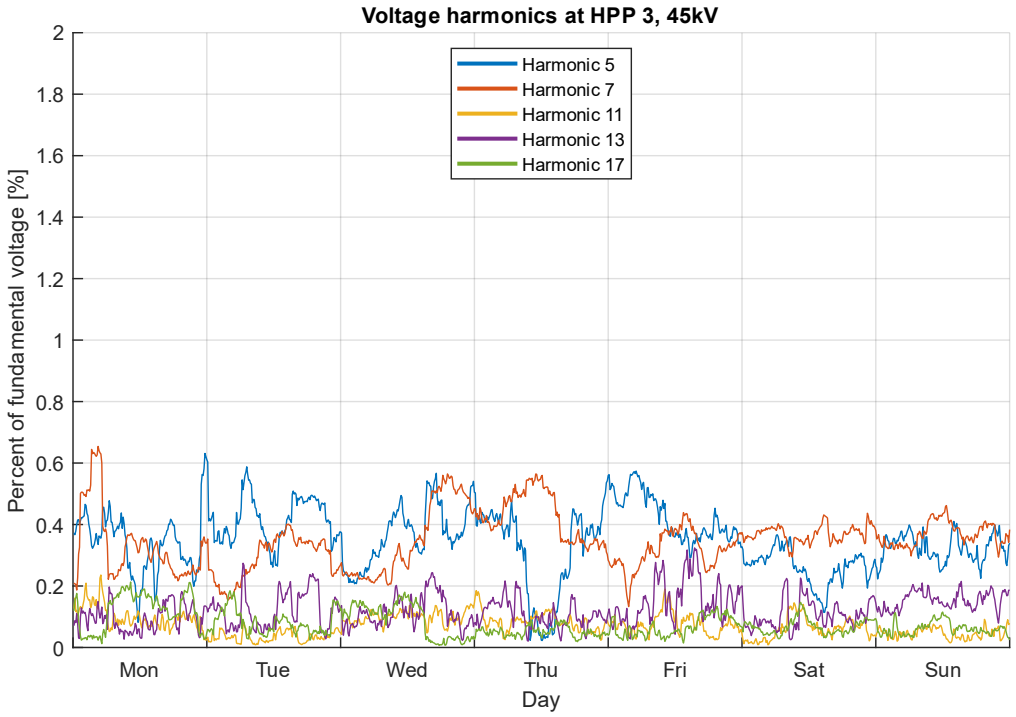

Figure 38 - Amplitude of the five first characteristic voltage harmonics at HPP 3 on the 45 kV bus.

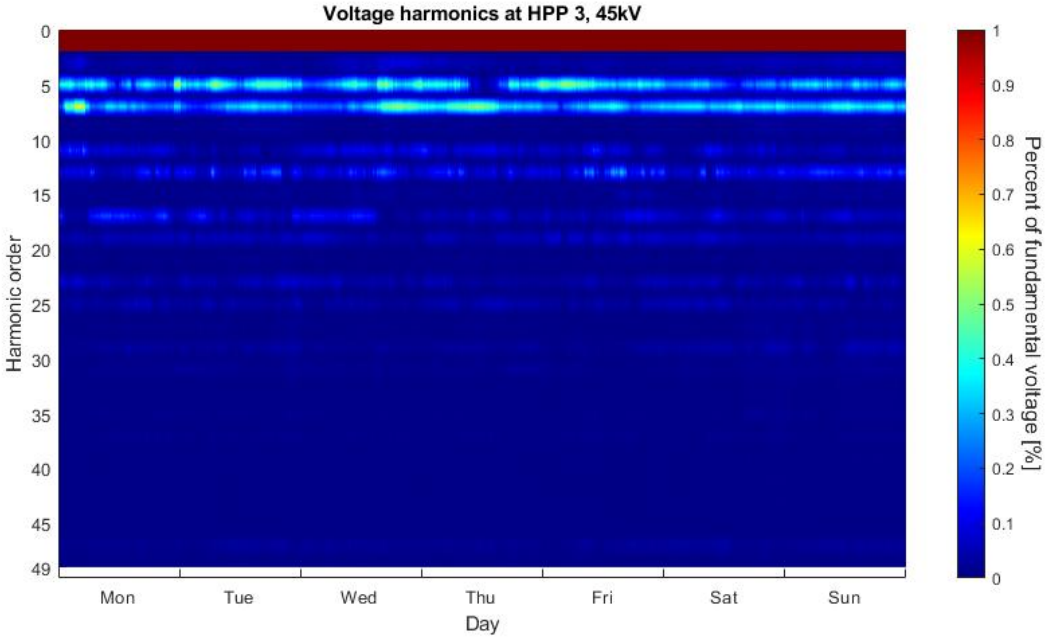

Figure 39 - Harmonic spectrum at HPP 3 on the 45 kV bus where the darkest red symbolizes a harmonic amplitude of 1% of fundamental or higher.

5.1.3.2 Measurements on the 220 kV bus

The measurements at the 220 kV bus cannot accurately guarantee the magnitude of the voltage harmonics due to the limitations of the CVT used, as explained in Section 2.5.2.2. Therefore, the results presented here should be considered indicative, as significant measurement errors may be present. Nevertheless, all voltage harmonics are below the limits specified by IEC

50160. The highest 10-minute average for each harmonic is shown in Table 7. Note that measurements were taken for harmonics 17, 19, 23, and 25, even though these do not have specific limits in IEC 50160. While IEC 50160 does not specify a limit for THD, IEEE 519 sets a THD limit of 1.5%, which is higher than the maximum THD of around 1.0% at the 220 kV bus. The THD for the entire week is shown in Figure 40.

Due to the significant uncertainties associated with the CVT's measurement accuracy, no detailed analysis of specific harmonics is presented. However, it is noted that the 13th harmonic is relatively large compared to the other HPPs included in this study. All harmonics can be seen in Figure 41 and Figure 42.

Table 7 - Compliance with IEC 50160 regarding individual harmonics at HPP 3 on the 220 kV bus. All values are presented as a percentage of the fundamental voltage. Significant measurement errors could exist since a CVT was used for measurement.

Odd harmonics						**Even harmonics**		
Not multiples of 3			**Multiples of 3**					
Order (h)	Limit (%)	Measured (%)	Order (h)	Limit (%)	Measured (%)	Order (h)	Limit (%)	Measured (%)
5	5,00	0,88	3	3,00	0,13	2	1,90	0,02
7	4,00	0,57	9	1,30	0,05	4	1,00	0,08
11	3,00	0,40	15	0,50	0,13	6 … 24	0,50	0,07
13	2,50	0,62	21	0,50	0,04			
17	-	0,37						
19	-	0,17						
23	-	0,10						
25	-	0,07						

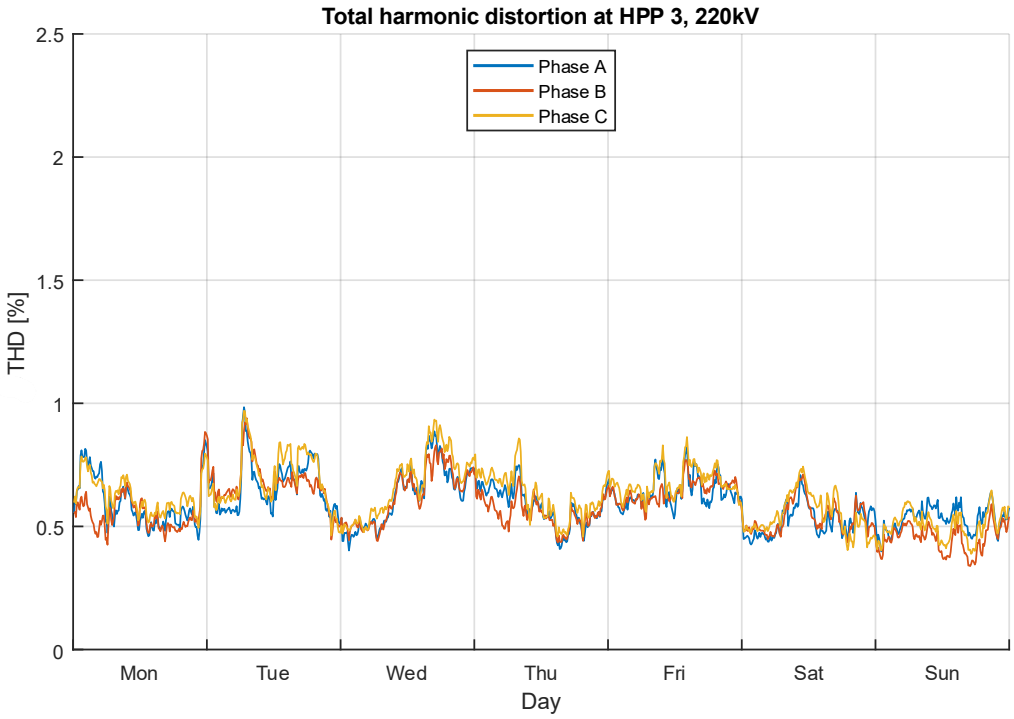

Figure 40 - THD of the voltage at HPP 3 on the 220 kV bus.

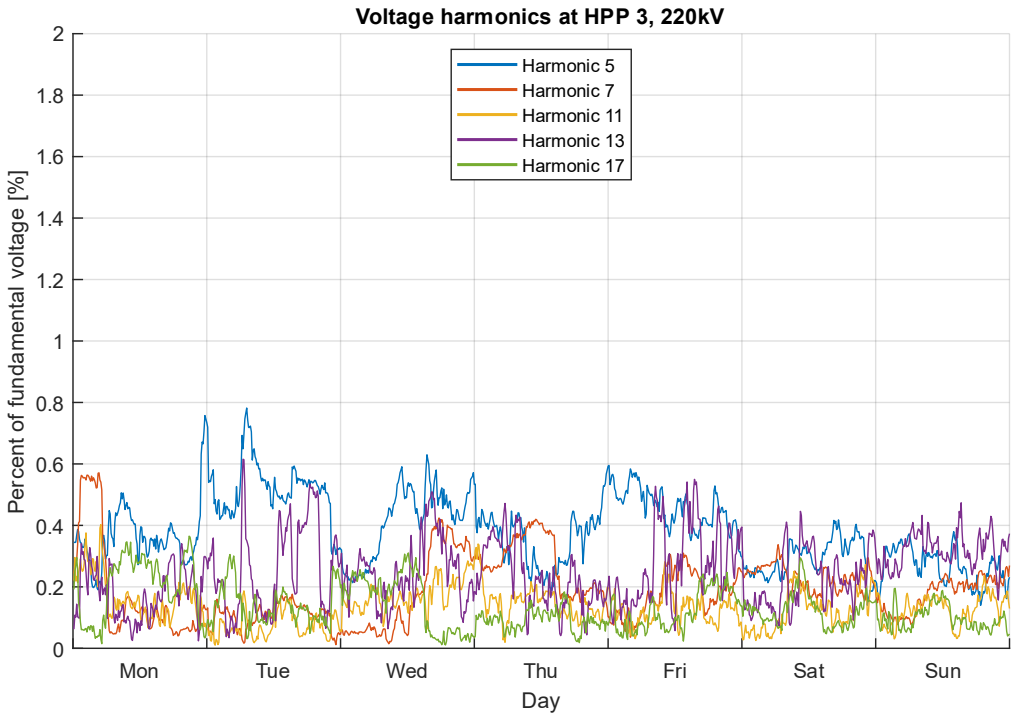

Figure 41 - Amplitude of the five first characteristic voltage harmonics at HPP 3 on the 220 kV bus.

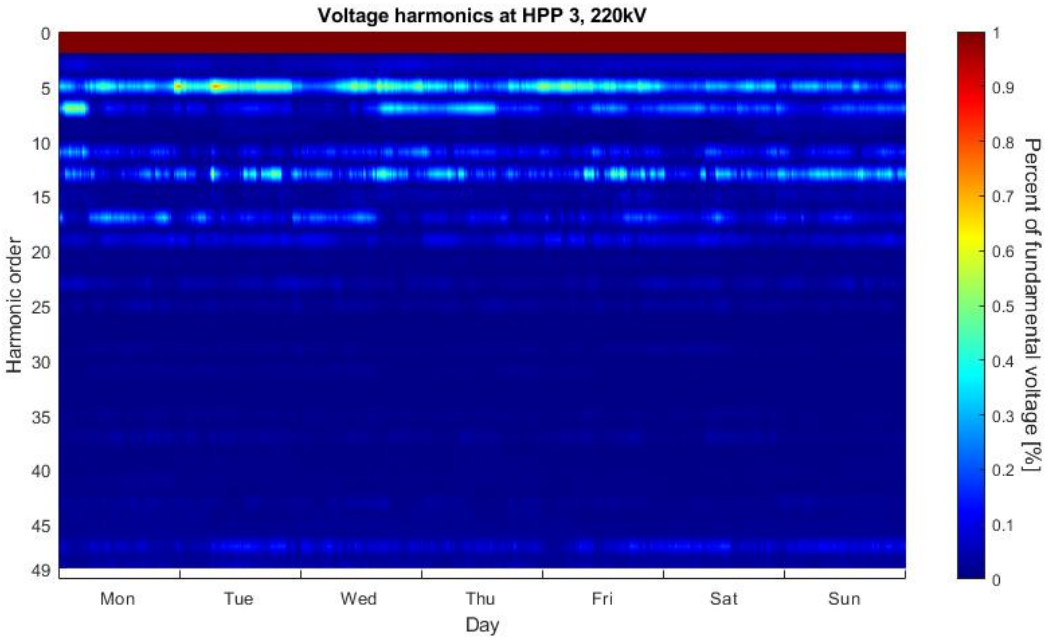

Figure 42 - Harmonic spectrum at HPP 3 on the 220 kV bus where the darkest red symbolizes a harmonic amplitude of 1% of the fundamental voltage or higher.

5.2 CURRENT MEASUREMENT

Current harmonics from a battery system were measured at HPP 4, up to a frequency of 10 kHz.

Figure 43 shows a FFT of the harmonic and supraharmonic currents up to a frequency of 10 kHz. The data is based on a saved waveform, recorded when the fundamental current was 103 A during a discharge of the battery. The figure indicates that all current harmonics were below 1% of the fundamental, except for the fifth harmonic. All supraharmonic currents were significantly smaller than the traditional harmonics. Note the difference in scale on the y-axis. Only a few supraharmonic components could be detected above the noise level around 0.005% of the fundamental current. The THD for the current was 2.55% for phase A, 2.19% for phase B, and 2.34% for phase C.

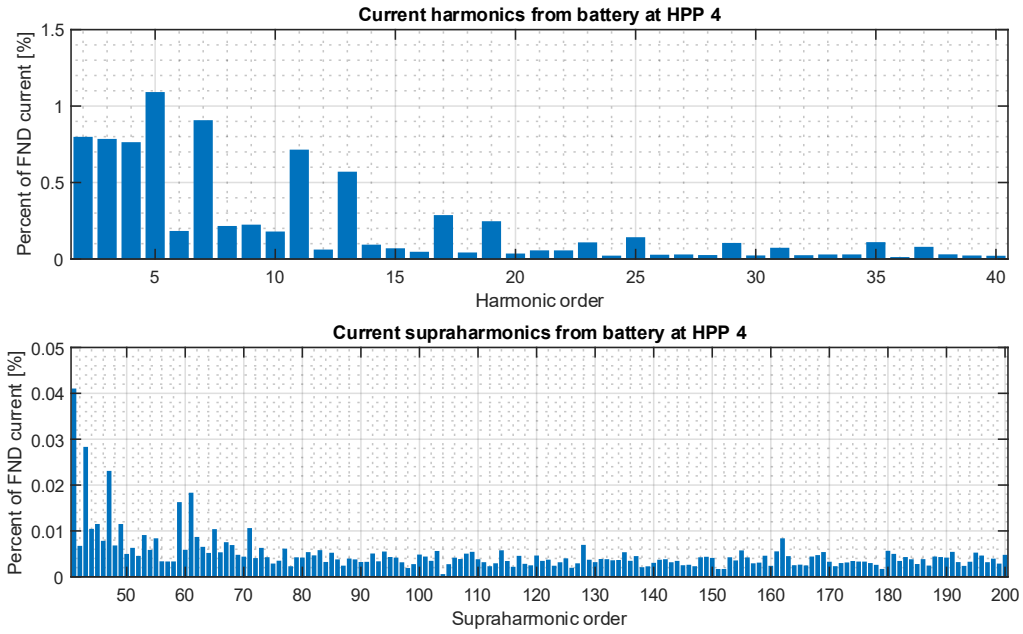

Figure 43 - FFT of the first 200 harmonics separated into two parts, when the battery was discharging with a fundamental current of 103 A. The upper one shows the first 40 harmonics, while the lower one shows the supraharmonics up to order 200. Note the difference in scale on the vertical axis between the two.

5.3 MEASUREMENT ERRORS

Measurement uncertainties in this thesis can be separated into two parts, uncertainties from the measurement transformers and uncertainties from the measurement instruments. The uncertainties of the measurement instruments are regarded as much smaller than the uncertainties of the measurement transformers used. Consequently, the error caused by the measurement instrument will be disregarded in this thesis, except for the current measurement at HPP 4. Since the accuracy of the measurement transformers for the voltage measurements was not possible to verify, Table 3 was used as a guideline for the error estimation.

5.3.1 HPP 1

For HPP 1, harmonic measurements with an accuracy of 1% are assumed to be possible up to the 50th harmonic according to Table 3. This means that the error limit of 5% stated in the standard IEC 61000-4-7 probably is fulfilled.

5.3.2 HPP 2

According to Table 3 can a good accuracy with a maximum error of 1% be assumed for harmonics up to the 20th harmonic. The accuracy between the 20th and 50th harmonic is however not clear, but based on the discussion in Section 4.4.1.2 is an assumption made that the maximum error is 20%.

5.3.3 HPP 3

At HPP 3, the IVT on the 45 kV bus is assumed to have an error below 1% up to the 20th harmonic according to Table 3. Above this frequency, the error is unknown, and data should be used with caution.

For the CVT on the 220 kV bus, the accuracy is more or less unknown for all harmonics except the fundamental frequency. No estimation of the error will be made.

5.3.4 HPP 4

The system for current measurement will differ a bit from the voltage measurements. In this evaluation, the errors occurring in the current sensor and the measurement instrument will be assessed.

The Dranflex 3000XLB current sensor has a frequency range from 10 Hz to 10 kHz with an attenuation of 1 dB at 10 kHz. The accuracy in the 300 A range is $\pm 1\%$ of the reading and $\pm 0.1\ A$. The reading from the measurement was 103 A, which can be found in Section 5.2. This gives a total measurement error for the current sensor of:

$$\pm 0.01 \cdot 103\ A \pm 0.1\ A = \pm 1.13\ A \text{ or } \pm\ 1.1\%.$$

The instrument has a sampling rate of 512 samples per cycle at fundamental frequency giving a sampling rate of 25.6 kHz which is more than twice the highest measured frequency of 10 kHz fulfilling the Nyqvist theorem described in Section 2.7. The accuracy of the measurement instrument is ± 0.1 % of reading ± 0.05 % of full scale. This gives an accuracy of:

$$\pm 0.001 \cdot 103\ A \pm 0.0005 \cdot 300\ A = \pm 0.253\ A \text{ or } \pm\ 0.25\%.$$

The maximum error is therefore the sum of the errors from the current sensor and the measurement instrument, which is:

$$\pm 1.13\ A + \pm 0.253\ A = \pm 1.383\ A \text{ or } \pm 1.34\%$$

Which is lower than the 5 % limit stated in IEC 61000-4-7. This is however just the maximum error of the sampled voltages. More errors can be added when the DFT and grouping/smoothing is performed, but those will be assumed to be small.

6 DISCUSSION

This section will discuss the results obtained from the measurements, including the problems with measuring voltage harmonics at high voltage levels. The literature review will also be further discussed.

6.1 MEASUREMENTS OF HARMONICS

A general conclusion across all HPPs is that the levels of voltage harmonics are well below the stated maximal levels according to the standard IEC 50160.

6.1.1 HPP 1

At HPP 1, a correlation between the fifth harmonic and weekdays from Monday to Friday is observed. This increase is caused by other sources of harmonics in the grid, as variation does not match any of the operations at the HPP. Both active and reactive power production remained almost constant at HPP 1, which can be seen in Appendix A.

The measurements conducted at HPP 1 indicate that there are no issues related to harmonics. Both the individual harmonics and the THD are well below the maximum level defined by IEC 50160. No significant levels of interharmonics were present.

6.1.2 HPP 2

At HPP 2 could the same be observed as in HPP 1, an increase of the fifth harmonic during weekdays. The increased fifth harmonic cannot be connected to any specific operations at HPP 2. The amplitude of the fifth harmonic is, however, well below the maximum levels according to IEC 50160 all the time.

Harmonic orders 25, 29, and 31 increase and decrease many times during the measurement period. Those variations match the production to the HPP connected to the same bus by a 50 km long overhead line. This line is only connected to two HPPs operated by Fortum, one of which was not in operation during the measurements. It could therefore be assumed that the operating HPP has an impact on harmonics 25, 29, and 31 at HPP 2. This could be caused by a harmonic source at the HPP or the fact that the connection of the synchronous generator at the HPP changed the grid impedance and therefore has an impact on the voltage harmonic levels at HPP 2. More measurement is required to draw definitive conclusions. The maximum voltage harmonic levels at HPP 2 for these three harmonics are still very low, including the assumed measurement error from the IVT.

There are similarities between voltage interharmonics at HPP 2 and measured current interharmonics in the paper by Yang et al. (2014) presented in Section 2.3.2.2. In the upper part of Figure 36, the average voltage interharmonics at HPP 2 is shown and that have similarities with, especially, turbine II in the paper by Yang et al. (2014). Turbine II is a DFIG with a rated power of 2 MW, similar to the type nearby HPP 2. Both have an increase of interharmonic five and seven together with an increase around the 50^{th} interharmonic or 2.5 kHz. One conclusion by Yang et al. (2014) is that interharmonics tend to be larger for higher frequencies which also was observed in the measurements at HPP 2. Figure 36 also present voltage interharmonics at HPP 2 during both high and low wind production. The

highest voltage interharmonics appears when wind production is high, and the voltage interharmonics almost disappears completely when wind production is low. This agrees well with another conclusions from Yang et al. (2014). Other conclusions from Yang et al. (2014) are not possible to confirm from the measurements at HPP 2. No limits on interharmonics exists in the standard IEC 50160, but Yang et al. (2014) shows that the current interharmonics at their measurements, for some frequencies exceed the current limit for the closest harmonic in the IEEE 519 standard. Part A.3 of the IEEE 519 standard presents values of maximum voltage interharmonics for guideline purposes. If sensitive equipment should be installed at a location where voltage interharmonics are present, the limits should be 0.1% in the subharmonic range, 0.2% around the fundamental frequency, 0.3% around odd harmonics and >0.3% around even harmonics. The amplitudes of the voltage interharmonics at HPP 2 are low and should therefore not cause any special problem even with the assumed measurement error of 20%.

The conclusion from the measurements at HPP 2 is that all harmonics covered in the standard IEC 50160 are within allowed levels and the highest harmonic distortion occurred during weekdays. There are harmonics and interharmonics with varying amplitudes at HPP 2 that may be associated with other sources such as wind power and a nearby HPP. A visible connection between interharmonics and wind power production can also be seen where the highest voltage interharmonics are found for the higher frequencies. Uncertainties of the IVT limit the accuracy of especially higher frequencies.

6.1.3 HPP 3

Voltage harmonics levels at HPP 3 are generally low, and any harmonics of extra interest cannot be found. The 45 kV IVT is assumed to have an acceptable accuracy up to the 20^{th} harmonic according to Table 3. No discussion from the 220 kV bus will be presented except that the harmonic levels probably were low compared to other measurement locations in this thesis.

The measurement data for the first 20 harmonics on the 45 kV bus do not show anything of interest. All voltage harmonics were low, and well below the limits.

The 13^{th} voltage harmonic on the 220 kV bus is larger than other harmonics, although it is typically smaller than the fifth harmonic. Xiao et al. (2004) presented a scenario where the 13^{th} harmonic is amplified in a CVT with a considerable amount. Figure 17 in Section 2.5.1.2 shows a comparison between the measurement from the CVT and a measurement on a capacitive tap on a current transformer. A similar situation might occur at HPP 4, but it cannot be verified without more measurements with an accurate voltage sensor. This type of problem could lead to situations where wrong conclusions are drawn, which can be costly if a failure occurs due to this.

6.1.4 Comparison between HPP 1 to 3

A conclusion can be drawn that proximity to higher voltage levels in the grid tends to reduce harmonic distortion levels in the grid. This is based on the THD levels at HPP 1, HPP 2, and HPP 3. The THD at HPP 1 and HPP 2 is around 1.5% according to Figure 27 and Figure 31 while the THD at HPP 3 is below 1% seen in Figure 37 and Figure 40. Additionally, it appears that grids with lower voltage levels are more susceptible to harmonic distortions caused by other equipment connected to the grid.

A general conclusion from the measurements is that no clear issue with voltage harmonics in the grids connecting Fortum's HPPs could be observed. However, it is important to take into account the uncertainties associated with the measurement transformers, which is a common limitation in this type of analysis.

6.1.5 Battery system at HPP 4

All measured harmonic currents were low, which aligns with expectations. The transformer located between the inverter and measurement point would attenuate many of the harmonics as partly described in Section 3.2. It was possible to see a small increase around the 60^{th} harmonic (3 kHz) as in the paper by Yaghoobi et al. (2020), presented in Section 3.3.1. This increase was small and barely above the background noise level in the measurements. The harmonics around the 60^{th} order are only causing around 0.01% of the losses compared to the fundamental current according to Equation 20, compared with 33% in the case described by Yaghoobi et al. (2020). It is however important to remember that the measurements at HPP 4 were performed on the primary side meaning that the current and THD are lower than on the secondary side due to the properties of the transformer explained in Equation 1.

There is also some difference between the current levels in the transformer at HPP 4 and the example by Yaghoobi et al. (2020), described in Section 3.3.1. In their example, the current levels could be high for many hours during a sunny day while the high current in the transformer at HPP 4 only occurs for short periods, when the grid frequency deviates too much. This sporadic current flow will not cause as big heat losses as when it operates with high currents during long periods.

The conclusion from the measurements at HPP 4 is that no tendency for problems could be found. A different result might have been obtained if the measurements could have been carried out on the secondary side of the transformers where the currents are higher.

6.2 MEASUREMENT TECHNIQUES

This section discusses the challenges of conducting accurate measurements in this thesis and offers recommendations for improving these methods in future studies.

6.2.1 Inaccuracy of measurement transformers

A recurring challenge throughout this thesis has been to find measurement points with sufficiently high accuracy. It was not possible to verify the accuracy of the measurement transformers used and all error approximations are based on other sources, such as Table 3, that at least gave some guidelines on when the IVT could be used. However, these are only guidelines and do not guarantee accurate measurements. To improve the quality of these measurements, a more accurate voltage sensor would be needed. An attempt was made to obtain a CVD for the measurements in the thesis, but it was unsuccessful. The idea of using a capacitive tap as a voltage sensor was considered but ultimately rejected. The biggest problem with the capacitive tap was gathering enough knowledge and resources in a short period of time to be able to perform the measurements in a safe way. This should optimally first be performed in a controlled laboratory environment, meaning that less time would be left for the measurements on site.

As standard measurement transformers were used, exact voltage harmonic levels cannot be guaranteed. It was assumed that errors of up to approximately 20% may be present for harmonics up to 2.5 kHz when IVTs were used in this thesis. For the CVT at HPP 3, errors exceeding 100% may occur even at frequencies of a few hundred hertz.

6.2.2 Measurement techniques for high frequencies

Harmonic measurement on MV levels and above requires specialized techniques and equipment. Depending on the purpose, and available equipment on-site, different methods can be more suitable. Based on the theory presented in Section 2.6, recommendations will be provided for different measurement techniques suitable for various voltage levels.

6.2.2.1 Measuring on HV and EHV systems

Since IVTs at HV and EHV generally have a low critical frequency according to Table 3, measurements of voltage harmonics are generally not recommended. CVTs perform even worse and are not recommended for any measurement except for the fundamental voltage. Other techniques are therefore a necessity for measuring voltage harmonics on these voltage levels

For the best measurement accuracy, a purpose built RCVD should be used. This will give the most accurate measurement with a high frequency range. The drawback is the high cost compared to other solutions.

For a temporary and cheaper measurement, the capacitive tap is a good alternative. This approach allows for a measurement with a high frequency range without investing in a costly RCDV that may otherwise be needed for such measurements.

A PQ sensor for CVTs can be a practical and cost-effective solution when a permanently mounted measurement system is desired. The drawback is however that it cannot be used with an IVT and does not have the same frequency range as a RCVD or a capacitive tap.

6.2.2.2 Measuring on MV systems

At the lower MV level of 10 kV, the critical frequency of IVTs is often sufficiently high to allow measurements up to the 50^{th} harmonic according to Table 3. Specially designed IVTs also exist with an extended frequency range of up to 10 kHz. However, when the voltage and frequency increase further, other methods are necessary.

A RCVD is also the optimal solution when high accuracy is required. Since the voltage levels are lower, it is possible to make the sensors smaller and cheaper. The smaller size also makes them easier to install in practical locations.

Measuring voltage harmonics on a capacitive tap and with PQ sensors on CVT at MV levels is challenging. This is because current transformers and bushings generally do not need a condenser core for field control since the voltage levels and electric fields are lower (Murty, 2017). For MV applications, IVTs are the primary choice of measurement transformers, which eliminates the option to use PQ sensors for CVTs.

6.3 RISK OF SUPRAHARMONICS AT HPPS

Supraharmonics are present in the electric grid and are expected to increase as more frequency converters are utilized. The most significant issues appear to occur in the LV grid near frequency converters. Supraharmonics are present in the MV grid as well; however, only a few cases when these have caused problems in higher voltage levels have been found in this thesis. Those that have been found in this thesis are located near a large source of supraharmonics. For instance, the failure of the cable termination explained in Section 3.3.2 took place at a converter station. The failure of the cable termination was an extreme case since the supraharmonic voltage levels reach up to 40% of the fundamental voltage, which is really high. An educated guess is that these types of problems likely do not pose a significant risk for HPPs today. However, the risk cannot be entirely dismissed. In the future, the number of supraharmonic sources is expected to increase. Studies have been conducted on whether wind- and solar power can be integrated to the same grid connection point as existing HPPs (Lindh, 2024). This might increase the possibility for significant emissions of supraharmonics in the vicinity of HPPs that can cause problems.

However, a suitable measurement system is essential for detecting supraharmonics. Without it, the problem may remain hidden, leading to increased losses and potentially causing unexplained failures.

6.4 FUTURE STUDIES

This thesis has provided only an overview of the topic, and many questions remain unanswered. A general recommendation for future research is to conduct additional measurements to deepen the understanding of harmonics in power systems. Traditional measurement transformers are limited even for harmonics up to 2 kHz. Future studies should therefore incorporate better measurement equipment, such as RCVDs, CVDs, or to use a capacitive tap. These approaches would provide more accurate data and enable a better picture of the harmonic contents in the grids connecting Fortum’s HPPs.

7 CONCLUSION

This thesis has investigated how harmonics can cause problems for electrical equipment at HPPs. Harmonic measurements at HPPs combined with literature reviews have been performed to be able to answer the research questions stated in Section 1.2.

In RQ1, the impact of harmonics on electrical equipment was investigated. Heat loss in equipment is the main issue with harmonics in the power system. Those heat losses can, in addition to decreasing efficiency, cause accelerated aging as well as failures in the worst case. Since all measurements in this thesis show low levels of harmonics, no specific problem could be observed. Supraharmonics may become an increasing problem for electrical equipment in the future due to the increased use of power converters in the grid. Supraharmonics can, due to their high frequency, generate significant heat losses even at low amplitudes.

Regarding RQ2, measurements of harmonic and supraharmonic voltages at higher voltage levels are difficult. Traditional measurement transformers generate large errors when the frequency increases. IVTs might give a reasonable low error for lower voltages and frequencies. For higher frequencies or voltages or if a CVT is utilized, other techniques are required. Three different techniques to measure voltage harmonics and supraharmonics have been presented in this thesis.

Measurement data from the HPPs reveals that voltage harmonic levels can vary during a week, which answers the last research question RQ3. Grids with lower voltage levels showed the largest variations of harmonics while less variation was visible at higher voltage levels. Correlations were observed between levels of voltage harmonics and the operation of other grid connected facilities, such as wind farms and neighboring HPPs. It was also possible to see voltage interharmonics that showed correlation with power production at a wind farm located 13 km away. All harmonic levels were however well below stated limits in the standard IEC 50160 and no clear risks for equipment at HPPs could be found. The measurements were however performed on regular measurement transformers, and uncertainties in the results are therefore expected.

REFERENCES

ABB (2015). *Instrument Transformers Application Guide*. ABB AB.

Akin, Firat and Arikan, Oktay (2023). The effect of thermal aging on solid insulating materials: A case study for dielectric loss and dissipation factor based evaluations under different voltage levels and frequencies. *Engineering Failure Analysis*, 148, p. 107222, doi:10.1016/j.engfailanal.2023.107222.

Alizade, Alireza and Noshahr, Javad Behkesh (2017). Evaluating noise and DC offset due to inter-harmonics and supra-harmonics caused by back-to-back converter of (DFIG) in AC distribution network. *CIRED*, 2017(1), p. 629–632, doi:10.1049/oap-cired.2017.0045.

Analog Devices (n.d.). Pulse Width Modulation. https://www.analog.com/media/en/training-seminars/design-handbooks/tutorial-ac-induction-permanent-magnet/Part1-Chapter4.pdf.

Anuar, M. N. K., Ismail, D., Indra, N. and Hafiz, A. M. (2012). Different total harmonic distortion effects on current transformer performance, 6.

Artale, Giovanni, Caravello, Giuseppe, Cataliotti, Antonio, Cosentino, Valentina, Ditta, Vito, Di Cara, Dario, Panzavecchia, Nicola, Tinè, Giovanni, Dipaola, Nunzio and Sambataro, Marilena G. (2022). Measurement issues on harmonic analysis according to the IEC 61000-4-7. In: *Proceedings of the 25th IMEKO TC4 International Symposium and 23rd International Workshop on ADC and DAC Modelling and Testing*. Presented at the 25th IMEKO TC4 International Symposium and 23rd International Workshop on ADC and DAC Modelling and Testing, Brescia, ITALY: IMEKO, p. 187–192.

Ashrafpour, Auob and Shahgholian, Ghazanfar (2020). HARMONICS GENERATED BY HYDROELECTRIC POWER PLANTS AND WIND FARMS IN THE POWER SYSTEM.

Austerlitz, Howard (2003). CHAPTER 4 - Analog/Digital Conversions. In: Austerlitz, Howard (ed.) *Data Acquisition Techniques Using PCs (Second Edition)*. San Diego: Academic Press, p. 51–77. https://www.sciencedirect.com/science/article/pii/B9780120683772500048.

Banerjee, Sarajit (2008). *A Study of High Frequency Voltage Effects in Medium Voltage Cable Terminations*. https://core.ac.uk/reader/144142740 [Accessed: 2025-04-28].

Behkesh Noshahr, Javad (2016). Emission phenomenon of supra-harmonics caused by switching of full-power frequency converter of wind turbines generator (PMSG) in smart grid. In: *2016 IEEE 16th International Conference on Environment and Electrical Engineering (EEEIC)*. Presented at the 2016 IEEE 16th International Conference on Environment and Electrical Engineering (EEEIC), p. 1–6.

Benjamin, Ankita and Jain, Sachin Kumar (2018). A Review of Literature on Effects of Harmonics on Protective Relays. In: *2018 IEEE Innovative Smart Grid Technologies - Asia (ISGT Asia)*. Presented at the 2018 IEEE Innovative Smart Grid Technologies - Asia (ISGT Asia), p. 407–412.

Boylestad, Robert L. (2016). *Introductory circuit analysis*. Thirteenth edition. Boston: Pearson.

Breeze, Paul (2016). Drive Trains, Gearboxes, and Generators. In: *Wind Power Generation*. Elsevier, p. 41–48. https://linkinghub.elsevier.com/retrieve/pii/B9780128040386000050.

BVM Systems Limited (n.d.). PQSensor^{TM} Broadband Voltage Transducer. http://bvmsystems.co.uk/Downloads_files/PQSensor_1.0_A4.pdf.

Carlsson, Jonny, Holmberg, David and Östlund, Jan (n.d.). NEW TECHNOLOGY FOR PQ MEASUREMENTS USING AUTO-CALIBRATION ON CAPACITIVE TAP ON INDUCTIVE CURRENT TRANSFORMERS.

Cigré (ed.) (2014). *Guidelines for power quality monitoring: measurement locations, processing and presentation of data*. Paris: CIGRÉ.

Dewayalage, Imanka (2025). *An on-site calibration system for high frequency harmonic voltage measurements in high voltage power systems*. Thesis. University of Wollongong. https://ro.uow.edu.au/articles/thesis/An_on-site_calibration_system_for_high_frequency_harmonic_voltage_measurements_in_high_voltage_power_systems/28180232/1.

Dewayalage, Imanka, Robinson, Duane A., Elphick, Sean and Perera, Sarath (2024). Measurement of High-Frequency Voltage Harmonics above 2 kHz in High-Voltage Networks. *Energies*, 17(4), p. 892, doi:10.3390/en17040892.

Douglass, D. A. (1981). Potential Transformer Accuracy at 60HZ Voltages Above and Below Rating and at Frequencies Above 60 HZ. *IEEE Transactions on Power Apparatus and Systems*, PAS-100(3), p. 1370–1375, doi:10.1109/TPAS.1981.316610.

Duan, Ruimin, He, Jie, Guo, Cheng and Zhou, Fulin (2021). Supraharmonics Transfer Characteristics of Transformer. In: *2021 IEEE 16th Conference on Industrial Electronics and Applications (ICIEA)*. Presented at the 2021 IEEE 16th Conference on Industrial Electronics and Applications (ICIEA), p. 1226–1231.

Eghtedarpour, N., Karimi, M. A. and Tavakoli, M. (2014). Harmonic resonance in power systems - a documented case. In: *2014 16th International Conference on Harmonics and Quality of Power (ICHQP)*. Presented at the 2014 16th International Conference on Harmonics and Quality of Power (ICHQP), p. 857–861.

EIA (2023). *Hydropower explained - U.S. Energy Information Administration (EIA)*. https://www.eia.gov/energyexplained/hydropower/ [Accessed: 2025-05-16].

Elfving, Gunnar (1993). *ABB HANDBOK INDUSTRI*. Västerås: ABB Industrigruppen.

Elsäkerhetsverket (2025). *EMC and products*. Elsäkerhetsverket. https://www.elsakerhetsverket.se/en/professionals/manufacturers-importers-and-distributors/the-different-product-requirements/emc-and-products/ [Accessed: 2025-05-17].

Energimarknadsinspektionen (2024). *Så här är elnätet uppbyggt*. Energimarknadsinspektionen. https://ei.se/konsument/el/sa-har-ar-elnatet-uppbyggt [Accessed: 2025-05-15].

Energimyndigheten (2023). *Scenarier över Sveriges energisystem 2023*. Energimyndigheten.

Espín-Delgado, Ángela, Letha, Shimi Sudha, Rönnberg, Sarah K. and Bollen, Math H. J. (2020). Failure of MV Cable Terminations Due to Supraharmonic Voltages: A Risk Indicator. *IEEE Open Journal of Industry Applications*, 1, p. 42–51, doi:10.1109/OJIA.2020.2998000.

FlirSystems (2021). USING ACOUSTIC IMAGING FOR PARTIAL DISCHARGE MONITORING. https://flir.netx.net/file/asset/35846/original.

Ghorbani, M. Jawad and Mokhtari, H. (2015). Impact of Harmonics on Power Quality and Losses in Power Distribution Systems, 5(1).

Glover, J. Duncan, Overbye, Thomas J. and Sarma, Mulukutla S. (2017). *Power system analysis & design*. Sixth edition. Boston, MA: Cengage Learning.

Gustavsson, Reidar (2003). *Praktisk elkvalitet*. 1. uppl. Borlänge: Norbo kraftteknik AB.

Higinbotham, William (2019). *MV Cable Termination Failure Prevention*.

IEC (2002). *Electromagnetic compatibility (EMC) – Part 4-7: Testing and measurement techniques*.

IEC (2011). *IEC 61869-5 Instrument transformers - Part 5: Additional requirements for capacitor voltage transformers*.

IEC (2022). *EN 50160:2022 Voltage characteristics of electricity supplied by public electricity networks*.

IEEE (1992). IEEE Standard Definitions for Power Switchgear. *IEEE Std C37.100-1992*, p. 1–82, doi:10.1109/IEEESTD.1992.106978.

IEEE (2021). IEEE Guide for Selection and Application of Terminations for Shielded AC Power Cable Rated 5 kV to 46 kV. *IEEE Std 1637-2020 (Revision of IEEE Std 1637-2010)*, p. 1–54, doi:10.1109/IEEESTD.2021.9351807.

IEEE (2022). *519 IEEE Standard for Harmonic Control in Electric Power Systems*. IEEE.

Kroposki, Ben (2024). *Introduction to Grid Forming Inverters: A Key to Transforming our Power Grid*.

Letha, S. S., Bollen, M. H. J., Rönnberg, S. and Delgado, A. S. (2021). Propagation of supraharmonics in a medium-voltage network. In: *CIRED 2021 - The 26th International Conference and Exhibition on Electricity Distribution*. Presented at the CIRED 2021 - The 26th International Conference and Exhibition on Electricity Distribution, p. 638–642.

Lindh, Anton (2024). *OPTIMISATION OF HYBRID RENEWABLE ENERGY SYSTEMS*. KTH, Stockholm.

Liu, Gang, Guo, Yaxun, Xin, Yanli, You, Lei, Jiang, Xiaofeng, Zheng, Ming and Tang, Wenhu (2018). Analysis of Switching Transients during Energization in Large Offshore Wind Farms. *Energies*, 11(2), p. 470, doi:10.3390/en11020470.

Marz, Michael B. (n.d.). Interharmonics: What They Are, Where They Come From and What They Do.

Meyer, Jan, Stiegler, Robert, Elst, Micheal, Klatt, Matthias and Sperling, E. (2011). Accuracy of Harmonic Voltage Measurements in the Frequency Range up to 5kHz using Conventional Instrument Transformers. Presented at the 21st International Conference on Electricity Distribution, Frankfurt.

Murty, K. K. (2017). Fundamentals of condenser bushings. *TRANSFORMERS MAGAZINE*, Special Edition: Bushings, p. 30–37.

Nisja, Indra (2018). Performance of current transformer operate under harmonic condition and their effects on transformer differential protection. *MATEC Web of Conferences*, 159, p. 02075, doi:10.1051/matecconf/201815902075.

Novitskiy, Alexander, Schlegel, Steffen and Westermann, Dirk (2018). Analysis of supraharmonic propagation in a MV electrical network. In: *2018 19th International Scientific Conference on Electric Power Engineering (EPE)*. Presented at the 2018 19th International Scientific Conference on Electric Power Engineering (EPE), p. 1–6.

Novitskiy, Alexander, Schlegel, Steffen and Westermann, Dirk (2020). Estimation of Power Losses Caused by Supraharmonics. *E3S Web of Conferences*, 209, p. 07008, doi:10.1051/e3sconf/202020907008.

Paulsson, L., Ekehov, B., Halen, S., Larsson, T., Palmqvist, L., Edris, A. A., Kidd, D., Keri, A. J. F. and Mehraban, B. (2003). High-frequency impacts in a converter-based back-to-back tie; the Eagle Pass installation. *IEEE Transactions on Power Delivery*, 18(4), p. 1410–1415, doi:10.1109/TPWRD.2003.817724.

Rajkumar, Supraja, Balasubramanian, R. and Kathirvelu, Parkavi (2024). A Comprehensive Review on Supraharmonics—The Next Big Power Quality Concern. *Smart Grids and Sustainable Energy*, 9(1), p. 15, doi:10.1007/s40866-024-00195-4.

Shokrollahi, H. and Janghorban, K. (2007). Soft magnetic composite materials (SMCs). *Journal of Materials Processing Technology*, 189(1), p. 1–12, doi:10.1016/j.jmatprotec.2007.02.034.

Slangen, T., de Jong, E., Cuk, V. and Cobben, S. (2023). Transfer of supraharmonics through a MV/LV transformer. In: *27th International Conference on Electricity Distribution (CIRED 2023)*. Presented at the 27th International Conference on Electricity Distribution (CIRED 2023), p. 110–114.

Sperling, Erik and Schegner, Peter (2013). A possibility to measure power quality with RC-divider. In: *22nd International Conference and Exhibition on Electricity Distribution (CIRED 2013)*. Presented at the 22nd International Conference and Exhibition on Electricity Distribution (CIRED 2013), p. 1–4.

SvK (2024). *Sveriges elnät*. Svenska kraftnät. https://www.svk.se/om-kraftsystemet/oversikt-av-kraftsystemet/sveriges-elnat/ [Accessed: 2025-05-11].

SvK (2025). *Elstatistik*. Svenska kraftnät. https://www.svk.se/om-kraftsystemet/kraftsystemdata/elstatistik/ [Accessed: 2025-05-15].

Tenbohlen, S., Kattmann, C., BRÜGGER, T., SIEGEL, M., KONERMANN, M., JUNGE, E. and CHRISTIAN, J. (2018). Power Quality Monitoring in Power Grids focusing on Accuracy of High Frequency Harmonics.

TEquipment (2025). *FLIR Si124-PD - Industrial Acoustic Imaging Camera for Partial Discharge Detection | TEquipment*. https://www.tequipment.net/FLIR/Si124-PD/Acoustic-Imagers/ [Accessed: 2025-05-06].

Thunberg, Erik (2001). *On the Benefit of Harmonic Measurements in Power Systems*. Stockholm.

Wakileh, George J. (2003). Harmonics in rotating machines. *Electric Power Systems Research*, 66(1), p. 31–37, doi:10.1016/S0378-7796(03)00069-5.

Wiid, Gideon and van der Merwe, Paul (2007). IEC and CISPR Standards.

Wildi, Theodore (1991). *Electrical machines, drives, and power systems*. 2 ed. Englewood Cliffs, N.J: Prentice-Hall.

Worzyk, Thomas (2009). *Submarine power cables: design, installation, repair, environmental aspects*. Dordrecht ; London: Springer.

Xiao, Yao, Fu, Jun, Hu, Bin, Li, Xiaoping and Deng, Chunnian (2004). Problems of voltage transducer in harmonic measurement. *IEEE Transactions on Power Delivery*, 19(3), p. 1483–1487, doi:10.1109/TPWRD.2004.829947.

Yaghoobi, Jalil, Alduraibi, Abdulrahman, Martin, Daniel, Zare, Firuz, Eghbal, Daniel and Memisevic, Rizah (2020). Impact of high-frequency harmonics (0–9 kHz) generated by grid-connected inverters on distribution transformers. *International Journal of Electrical Power & Energy Systems*, 122, p. 106177, doi:10.1016/j.ijepes.2020.106177.

Yang, Kai, Bollen, Math H. J., Larsson, E. O. Anders and Wahlberg, Mats (2014). Measurements of harmonic emission versus active power from wind turbines. *Electric Power Systems Research*, 108, p. 304–314, doi:10.1016/j.epsr.2013.11.025.

Zhang, Dahai, Xu, W. and Liu, Yutian (2005). On the phase sequence characteristics of interharmonics. *IEEE Transactions on Power Delivery*, 20(4), p. 2563–2569, doi:10.1109/TPWRD.2005.852330.

Zhao, Li, H. Y., Ghassemi, F. and Crossley, P. (2010). Impact of Power Quality Sensor technique on power system protection voltage transient measurements. In: *10th IET International Conference on Developments in Power System Protection (DPSP 2010). Managing the Change*. Presented at the 10th IET International Conference on Developments in Power System Protection (DPSP 2010). Managing the Change, p. 1–4.

Zhao, S. P. (2013). *Design and Implementation of a Frequency Response Test System for Instrument Voltage Transformer Performance Studies*. The University of Manchester.

Zolett, Benhur and Leborgne, Roberto Chouhy (2020). Propagation of Supraharmonics Generated by PMSG Wind Power Plants into Transmission Systems. In: *2020 IEEE PES Transmission & Distribution Conference and Exhibition - Latin America (T&D LA)*.

Presented at the 2020 IEEE PES Transmission & Distribution Conference and Exhibition - Latin America (T&D LA), p. 1–6.

Zong, Wen-Zhi, Li, Yue, Cheng, Yang-Chun, Zhang, Chun-Yu, Xue, Yang and Li, Guan-Gmao (2010). The design of a wide-band high-voltage divider. In: *2010 International Conference on Power System Technology*. Presented at the 2010 International Conference on Power System Technology, p. 1–5.

Appendix A, Measurement data

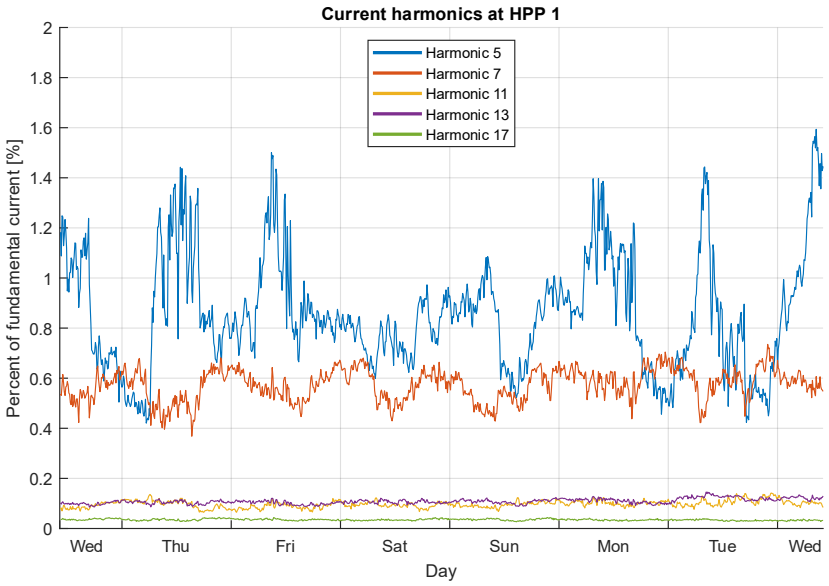

Figure A1 - Amplitude of the five first characteristic current harmonics at HPP 1.

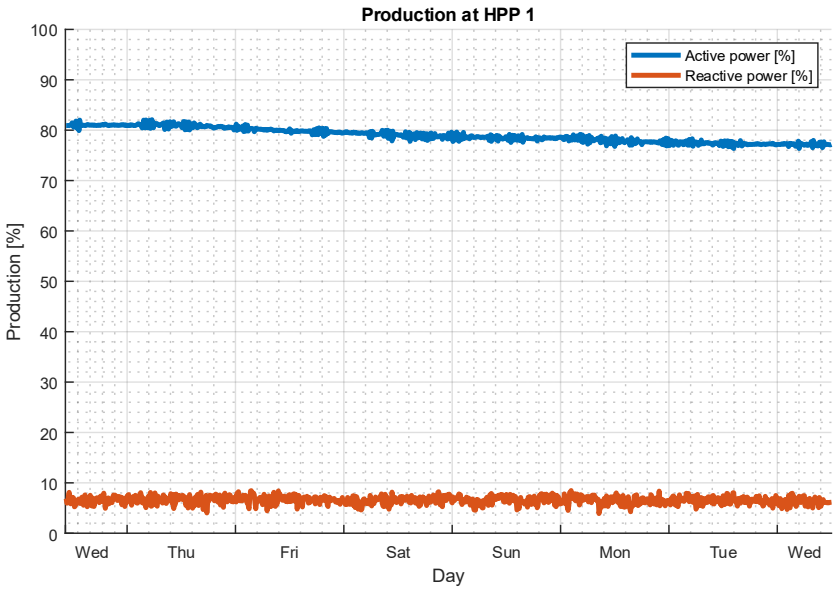

Figure A2 - Power production at HPP 1 normalized with an arbitrary value.

Appendix A

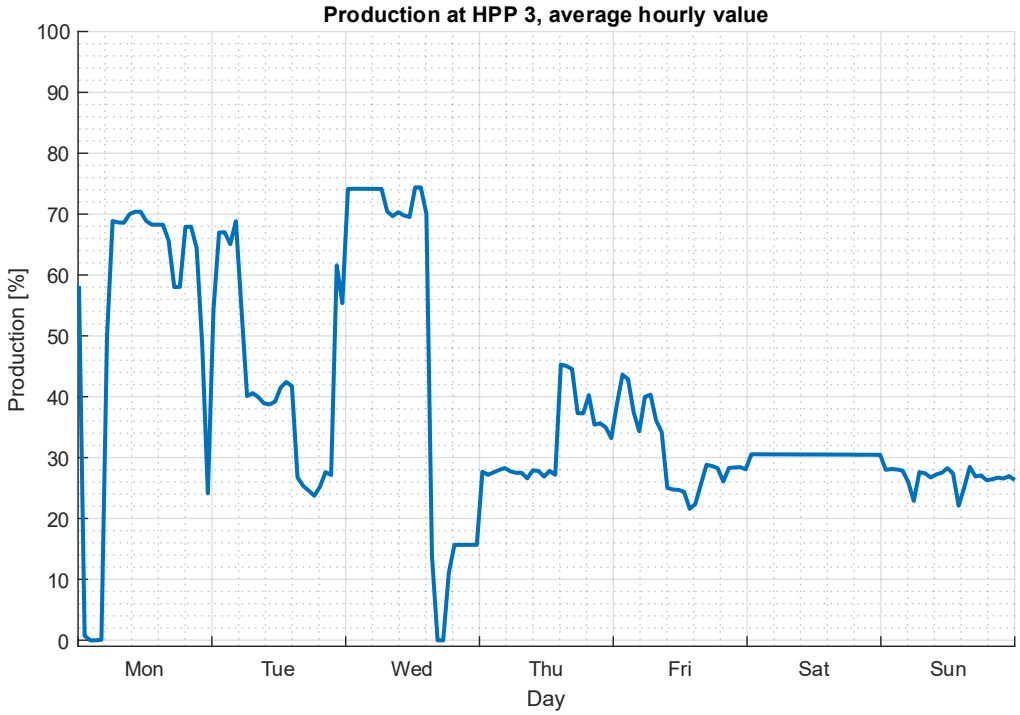

Figure A3 - Power production at HPP 3 normalized with an arbitrary value.

Appendix B, Standards

Table B.1 Allowed voltage harmonics for different voltage levels according to the standard IEC 50160. The values represent a percentage of the fundamental voltage (u.c stands for "under consideration").

Harmonic order [h]	LV(%)	MV(%)	HV(%)	EHV(%)
2	2	2	1,9	1,9
3	5	5	3	3
4	1	1	1	1
5	6	6	5	5
6	0,5	0,5	0,5	0,5
7	5	5	4	4
8	0,5	0,5	0,5	0,5
9	1,5	1,5	1,3	1,3
10	0,5	0,5	0,5	0,5
11	3,5	3,5	3	3
12	0,5	0,5	0,5	0,5
13	3	3	2,5	2,5
14	0,5	0,5	0,5	0,5
15	1	0,5	0,5	0,5
16	0,5	0,5	0,5	0,5
17	2	2	u.c.	u.c.
18	0,5	0,5	0,5	0,5
19	1,5	1,5	u.c.	u.c.
20	0,5	0,5	0,5	0,5
21	0,75	0,5	0,5	0,5
22	0,5	0,5	0,5	0,5
23	1,5	1,5	u.c.	u.c.
24	0,5	0,5	0,5	0,5
25	1,5	1,5	u.c.	u.c.